

115

1995120310

N95-26730

P 20

Peripheral Innervation Patterns of Vestibular Nerve Afferents in the Bullfrog Utriculus

R.A. BAIRD AND N.R. SCHUFF

Department of Neuro-otology and R.S. Dow Neurological Sciences Institute, Good Samaritan Hospital and Medical Center, Portland, Oregon 97209

ABSTRACT

Vestibular nerve afferents innervating the bullfrog utriculus differ in their response dynamics and sensitivity to natural stimulation. They also supply hair cells that differ markedly in hair bundle morphology. To examine the peripheral innervation patterns of individual utricular afferents more closely, afferent fibers were labeled by the extracellular injection of horseradish peroxidase (HRP) into the vestibular nerve after sectioning the vestibular nerve medial to Scarpa's ganglion to allow the degeneration of sympathetic and efferent fibers. The peripheral arborizations of individual afferents were then correlated with the diameters of their parent axons, the regions of the macula they innervate, and the number and type of hair cells they supply.

The utriculus is divided by the striola, a narrow zone of distinctive morphology, into medial and lateral parts. Utricular afferents were classified as striolar or extrastriolar according to the epithelial entrance of their parent axons and the location of their terminal fields. In general, striolar afferents had thicker parent axons, fewer subepithelial bifurcations, larger terminal fields, and more synaptic endings than afferents in extrastriolar regions. Afferents in a juxtastriolar zone, immediately adjacent to the medial striola, had innervation patterns transitional between those in the striola and more peripheral parts of the medial extrastriola. Most afferents innervated only a single macular zone. The terminal fields of striolar afferents, with the notable exception of a few afferents with thin parent axons, were generally confined to one side of the striola.

Hair cells in the bullfrog utriculus have previously been classified into four types based on hair bundle morphology (Lewis and Li: *Brain Res.* 83:35-50, 1975). Afferents in the extrastriolar and juxtastriolar zones largely or exclusively innervated Type B hair cells, the predominant hair cell type in the utricular macula. Striolar afferents supplied a mixture of four hair cell types, but largely contacted Type B and Type C hair cells, particularly on the outer rows of the medial striola. Afferents supplying more central striolar regions innervated fewer Type B and larger numbers of Type E and Type F hair cells. Striolar afferents with thin parent axons largely supplied Type E hair cells with bulbed kinocilia in the innermost striolar rows. © 1994 Wiley-Liss, Inc.

Key words: inner ear, otolith organ, hair cells, horseradish peroxidase

The peripheral innervation patterns of vestibular nerve afferents were first examined in pioneering silver stain studies (Ramón y Cajal, '08, '09; Lorente de Nó, '26; Poljak, '27). These studies revealed that the vestibular nerve is composed of fibers with a wide range of fiber diameters that supply different regions of the vestibular endorgans. In general, the thickest fibers in the vestibular nerve supply the most central regions of the vestibular endorgans, while more peripheral regions receive afferents with thinner parent diameters. In the vestibular otolith organs, this central region is the striola, a narrow zone of distinctive

morphology that runs the entire length of the sensory epithelium and divides it into medial and lateral parts (Werner, '33; Lindeman, '69; Wersall and Bagger-Sjoberg, '74).

More recently, intracellular and extracellular labelling techniques have been used in both mammals (Fernandez et al., '88, '90) and other vertebrates (O'Leary et al., '76;

Accepted August 4, 1993.

Address reprint requests to Dr. Richard A. Baird, R.S. Dow Neurological Sciences Institute, 1120 NW 20th Avenue, Portland, OR 97209.

Honrubia et al., '81, '89; Schessel and Highstein, '81; Lewis et al., '82; Baird and Lewis, '86; Boyle et al., '91; Myers and Lewis, '91; Schessel et al., '91) to examine afferent innervation patterns in individual vestibular endorgans and to correlate the peripheral innervation patterns of individual afferents with the regions of the endorgan they innervate and the number and types of hair cells they supply. In mammals, these studies have shown that the response dynamics of vestibular afferents are more closely related to their fiber diameter and location in the sensory epithelium than to their terminal morphology (Goldberg et al., '85; Baird et al., '88; Goldberg et al., '90b). Response sensitivity, on the other hand, is related to the number of Type I and Type II hair cells innervated by an afferent fiber.

Studies in lower vertebrates, in preparations in which all hair cells are Type II by cell body and synapse morphology (Wersall and Bagger-Sjockack, '74), have revealed a similar organizational principle (O'Leary et al., '76; Baird and Lewis, '86; Honrubia et al., '81, '89; Boyle et al., '91; Myers and Lewis, '91). These results suggest that differences in afferent sensitivity and response dynamics are the result of regional variations in presynaptic transduction mechanisms. In the semicircular canals, these differences may reflect regional variations in cupular membrane dynamics (Hillman and McLaren, '79; McLaren and Hillman, '79; Boyle et al., '91) or the coupling of the cupular membrane to hair cells in different epithelial locations (Lim, '76; Honrubia et al., '81, '89). In the otolith organs, on the other hand, differences in afferent sensitivity may be determined by transduction mechanisms within individual hair cells. In the bullfrog utricle, a number of subtypes of the Type II hair cell have been defined based on hair bundle morphology (Lewis and Li, '75). Morphophysiological studies in this endorgan have shown that the sensitivity of an afferent is correlated with both the macular location and the hair bundle morphology of its innervated hair cells (Baird and Lewis, '86; Myers and Lewis, '91).

The present study is part of a larger project in which intracellular recording techniques were used to characterize the physiological response properties of hair cells in the bullfrog utricular macula (Baird, '92, '93a,b). In this paper, afferent fibers supplying the utricular macula of the bullfrog were labeled by extracellular injections of HRP into the vestibular nerve after previously sectioning the nerve medial to Scarpa's ganglion to allow the degeneration of sympathetic and efferent fibers. The aim of these studies was to correlate the peripheral innervation patterns of individual afferents with the sizes of their parent axons, the regions of the endorgan they innervate, and the number and types of hair cells they supply.

Our results provide a context for recent companion studies (Baird, '92, '93a,b), in which we demonstrate that utricular hair cells differ in their voltage responses to intracellular current and hair bundle displacement. By revealing the relation between individual afferents and the number and types of hair cells they supply, they also suggest how differences in the transduction mechanisms of different hair cell types in the utricular macula might contribute to differences in sensitivity and response dynamics among vestibular afferents. Finally, our results extend the results of previously published morphophysiological studies (Baird and Lewis, '86; Myers and Lewis, '91). In these studies, intra-axonal labeling techniques were used to correlate the morphology and physiology of individual vestibular nerve afferents. Unfortunately, such studies are

only able to record from small samples of fibers and are highly biased towards sampling from large-diameter fibers. Using extracellular HRP techniques, we were able to label a larger, more representative sample of afferent fibers. In addition, afferents in earlier studies were labeled with the fluorescent dye Lucifer Yellow and their terminal arborizations reconstructed in wholemount preparations. It is difficult to identify hair cell types and to assess fully the terminal arbors of afferents under these conditions. These problems were circumvented in the present study by observing labeled afferents and unlabeled hair cells with Nomarski optics in both wholemount and sectioned material.

Preliminary accounts of portions of this data have been presented in abstract form (Baird, '91).

MATERIALS AND METHODS

Sectioning of the vestibular nerve

Eight bullfrogs (*Rana catesbeiana*), weighing 90–160 g, were anesthetized by immersion in 0.2% MS-222 (Sigma). With sterile technique, the right vestibular nerve was exposed intracranially through a small hole in the parasphenoidal bone and sectioned medial to Scarpa's ganglion to allow the degeneration of sympathetic and efferent fibers (Robbins et al., '67). Great care was taken during this procedure to avoid disturbance of the vasculature surrounding the vestibular nerve. Following surgery, the hole was packed with sterile Gelfoam. We then sutured the incision through the overlying muscle, applied topical anesthetic to the wound, and allowed bullfrogs to recover from the effects of the anesthetic. Upon recovering from anesthesia, bullfrogs initially displayed a tilting of the head toward the side of the lesion, an asymmetrical pose typical after unilateral labyrinthectomy, and made little or no active movements. Bullfrogs were placed in recirculating aquaria in a quiet, darkened room until they exhibited normal postural reflexes (normally 1–2 days) and then returned to normal lighting conditions.

Injection of horseradish peroxidase

After 10–14 days, a length of time sufficient to guarantee the degeneration of efferent vestibular fibers (Robbins et al., '67), bullfrogs were reanesthetized with 0.2% MS-222. The right vestibular nerve was reexposed and injected extracellularly with a solution of HRP. Dimethyl sulfoxide (DMSO) was added to the injection solution to facilitate the labeling of the terminal arbors of labeled afferent fibers (Keefer et al., '76; West and Black, '79). Thin-walled borosilicate micropipettes, broken to tip diameters of 30–50 μm , were filled with a solution of 20% HRP (Sigma, type VI) and 2% DMSO (Sigma) in 0.1 M phosphate buffer (pH 7.25). Typically, HRP was pressure injected at three sites across the anterior-posterior extent of the anterior branch of the right vestibular nerve. Following HRP injections, bullfrogs were repacked with Gelfoam, resutured, and allowed to recover from anesthesia.

Removal of the vestibular endorgans

Three days after HRP injection, animals were again reanesthetized with 0.2% MS-222, decapitated, and the anterior vestibular nerve and utricular macula from the injected side dissected from the membranous labyrinth in cold, oxygenated physiological saline. We then fixed the vestibular nerve and utricular macula overnight in 4.0% paraformaldehyde in 0.1 M phosphate buffer (pH 7.25).

After rinsing in fresh phosphate buffer, utricular maculae were separated from the vestibular nerve. The vestibular nerve was then embedded in glycol methacrylate (Polysciences, JB-4), serially cross-sectioned at 1 μm with a sliding microtome (LKB, Historange), and counterstained for 1 minute in 1% Toluidine Blue.

The otolith membranes of utricular maculae were removed by gentle mechanical agitation after a brief (30–45 minute) enzymatic digestion in 30 $\mu\text{g}/\text{ml}$ subtilopectidase BPN' (Sigma). A cobalt modification of the diaminobenzidine (DAB) procedure was then used to visualize HRP reaction product in the utricular macula (Adams, '77). To ensure penetration of reagents, maculae were preincubated for 30 minutes in 1% DMSO and an additional 30 minutes in 0.05% DAB, both in 0.1 M phosphate buffer. HRP reaction product was visualized by adding 0.015% cobalt chloride and 0.015% hydrogen peroxide to the above solution for an additional 10–20 minutes. Maculae were then dehydrated in an ethanol series, cleared briefly in xylene, and mounted in Eukit (Calibrated Instr.) on clean glass slides.

Morphological analyses

Material was examined with Nomarski optics with $\times 63$ and $\times 100$ oil-immersion objectives (Zeiss). We first compared Toluidine Blue-stained cross sections of the anterior vestibular nerve branchlet immediately proximal to the utricular macula in normal and nerve-sectioned animals. Myelinated axon profiles were divided into one of two classes: 1) normal axons; and 2) degenerated axons, defined as those axons whose volume of cytoplasmic material was <25% of their interior volume. Axons in the first group were assumed to be the axons of vestibular afferents; axons in the second group were assumed to be the remnants of vestibular efferents (Robbins et al., '67; Dunn, '78; Gacek, '84).

The possibility for direct counts or measurements of axon diameter for fibers supplying the utricular macula was precluded since no single plane contained all of these fibers in cross section. We therefore determined, in two normal and two nerve-sectioned animals, the number and axon diameter of the above two fiber classes in the anterior vestibular nerve and the horizontal and anterior vertical ampullary nerve branchlets by using a computerized image analysis program (Bioquant, System IV). For each fiber class, we estimated figures for the utricular macula by subtracting the number of ampullary nerve fibers from the number of fibers in the anterior vestibular nerve. Individual axon diameters were multiplied by a normalization factor (see below), averaged to obtain mean values, and sorted into 0.05 μm bins.

Using the Bioquant image analysis system, we drew the macular outline and the borders of the striolar region for each wholmount macula. The entrance of each labeled axon into the sensory epithelium was indicated on a standard surface map of the utricular macula determined by overlaying the striolar regions of the utricular maculae in four nerve-sectioned animals. The size of each parent axon was obtained by averaging its axolemmal diameter, measured every 10 μm , starting from the basement membrane and continuing proximally for 100 μm or as far as the axon could be traced. For afferents that bifurcated below the sensory epithelium, the entrance of the thickest branch was used to define the unit's epithelial location and measurements of axolemmal diameter began proximal to the first

branch point. The terminal field of an afferent was defined by the total extent of its peripheral arborization in the horizontal plane. The surface area of the sensory macula was used to normalize for differential shrinkage between specimens. For each macula, axon diameters and terminal-field dimensions were multiplied by a normalization factor, $(A_m/A_i)^{1/2}$, where A_i is the area of a particular epithelium and A_m is the mean area of $0.554 \pm 0.003 \text{ mm}^2$ (mean \pm SEM) for a sample that included four maculae from normal animals and four maculae from nerve-sectioned animals.

To examine terminal morphology and the intraepithelial distribution of synaptic endings more closely, wholmount utricular maculae were embedded in glycol methacrylate (Polysciences, JB-4) and serially sectioned at 10–20 μm in a coronal plane. The plane of section is shown in Figure 1a. The size of the parent axons and the terminal fields of labeled afferents were confirmed in sectioned material. The complete peripheral arborizations of well-isolated afferents were then reconstructed in their entirety from serial sections and drawn with a camera lucida (total magnification $\times 1,800$). With Nomarski optics, the number and type of hair cells contacted by well-labeled afferents were determined by examining the relationship between their terminal endings and individual hair cells.

Utriclar hair cells, following the original scheme of Lewis and Li ('75), were classified into four types according to the size of their hair bundles, the absence or presence of a bulbed kinocilium, and the relative lengths of their kinocilium and tallest stereocilia (Fig. 1b,c). Type B cells, the predominant hair cell type in the utricular macula, had small hair bundles and short stereocilia, with kinocilia 2–6 times as long as their tallest stereocilia. These cells were found throughout the medial and lateral extrastriola and, more rarely, in the striolar region. Three other hair cell types, with stereocilia markedly longer than those of Type B cells, were confined to the striolar region. Type C cells, concentrated in the outer striolar rows, resembled enlarged Type B cells, having kinocilia and stereocilia approximately twice as long as the latter hair cell type. Moving inward, these cells were gradually replaced by two hair cell types with kinocilia approximately equal in length to their tallest stereocilia, significantly shorter than the kinocilia of Type B and Type C cells. Type F cells had visibly larger hair bundles than other utricular hair cells. Type E cells, restricted to the innermost striolar rows, had somewhat smaller hair bundles and, unlike Type F cells, possessed prominent kinociliary bulbs.

Unless otherwise stated, statistical comparisons of morphometric data were based on a one-way analysis of variance (ANOVA). When appropriate, post hoc pairwise multiple comparisons were performed using the Tukey multiple comparison test adjusting, when necessary, for unequal group sizes (Miller, '77).

RESULTS

Organization of the vestibular nerve

A Toluidine Blue-stained cross section of the anterior vestibular nerve branchlet immediately medial to the utricular macula in a normal animal is illustrated in Figure 2a. The stained nuclei of Schwann cells (black profiles) and the myelin sheath and interior cytoplasm of myelinated fibers are clearly seen. Myelinated fibers in the nerve branchlet had a wide variety of axolemmal diameters, ranging from

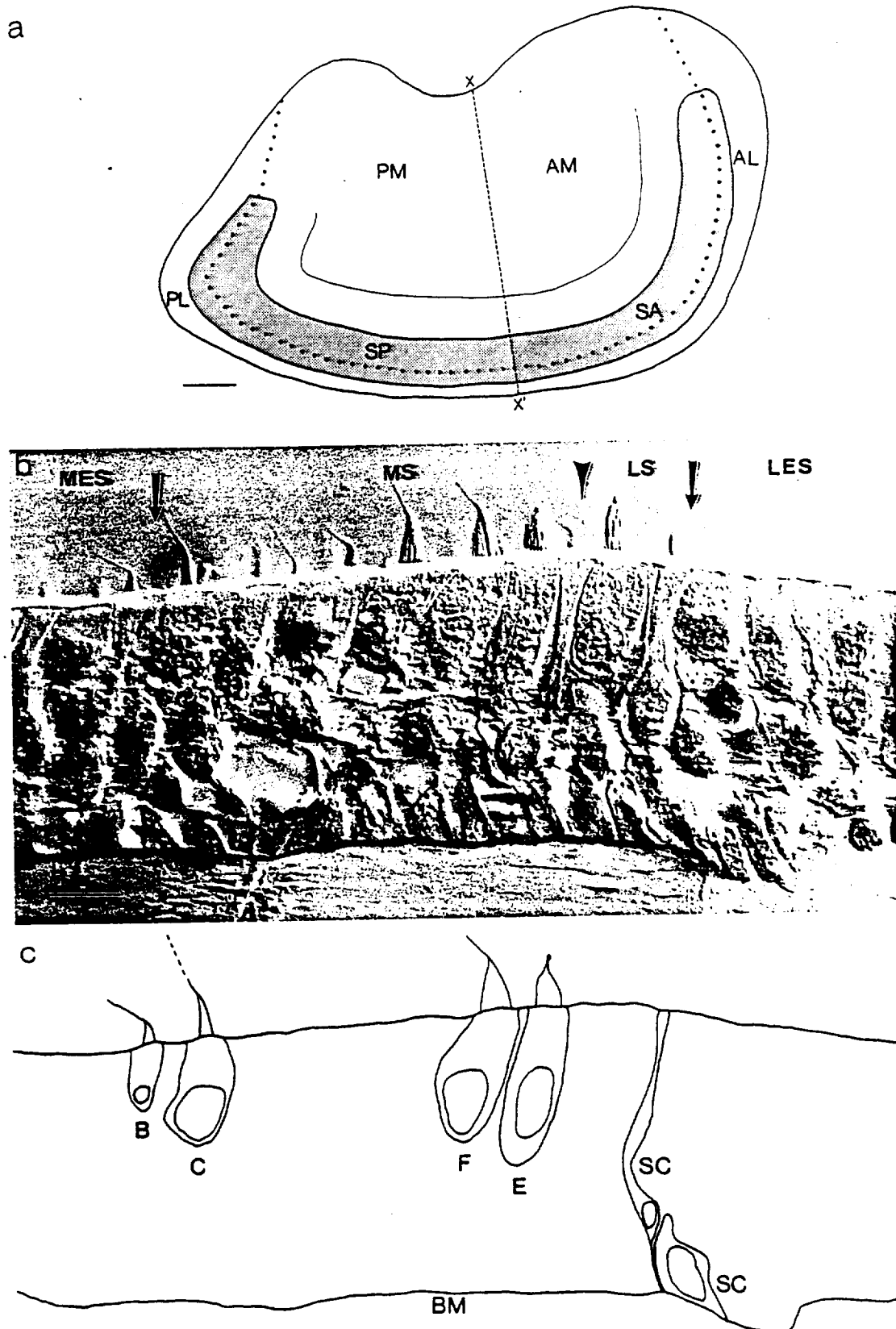


Fig. 1. a: Standard surface map of the utricular macula based on 8 maculae. The striola (shown shaded), a thin ribbon-shaped area, and its anterior and posterior extensions (dotted lines) separate the extrastriola into a larger medial and a smaller lateral zone. Thin solid line indicates the border of the juxtastricular region. A dashed line (x--x') divides the macula into anterior and posterior halves and indicates the plane of section seen below and in Figure 3. AL, anterolateral extrastriola; AM, anteromedial extrastriola; PL, posterolateral extrastriola; PM, posteromedial extrastriola; SA, anterior striola; SP, posterior striola. b: Photomicrograph of Toluidine Blue-stained cross section of

the utricular striola and surrounding extrastricular regions. Arrows denote the medial (left) and lateral (right) borders of the striolar region; arrowhead indicates the reversal of hair cell polarization. MES, medial extrastriola; MS, medial striola; LS, lateral striola; LES, lateral extrastriola. c: Schematic sketch of section in b, indicating the intraepithelial location and cellular morphology of representative hair cells and supporting cells in the utricular macula. B, Type B; C, Type C; E, Type E; F, Type F; SC, supporting cell; BM, basement membrane. Bars = 100 μ m in A, 25 μ m in B.

0.2 to $> 5 \mu\text{m}$. The great majority of fibers innervating the utricular macula had axolemmal diameters lying between 0.3 and $0.5 \mu\text{m}$ (Fig. 2c). Two degenerated myelinated fibers (not shown in Fig. 2) were recognizable by their lack of cytoplasmic material. A substantial number of unmyelinated fibers, primarily in the central portion of the nerve branchlet, were also observed. The axolemmal diameters of these fibers were invariably smaller than those of myelinated axons and could not be reliably measured in the light microscope. Large numbers of these fibers were also seen outside the lateral macular margins in wholemount utriculus preparations. These fibers did not enter the sensory epithelium and were observed in close proximity to blood vessels. They were therefore assumed to be the axons of sympathetic fibers (Lindeman, '69; Dunn, '78).

The anterior vestibular nerve branchlets of nerve-sectioned animals, as in normal animals, were composed of myelinated fibers with widely varying axolemmal diameters (Fig. 2b). The interior cytoplasm of many afferents in nerve-sectioned animals were dark in appearance, indicating that they were labeled with horseradish peroxidase (pointers, Fig. 2b). The axolemmal diameters of myelinated fibers were similar in normal (Fig. 2c) and nerve-sectioned (Fig. 2d) animals. In two other respects, the nerve branchlets of nerve-sectioned animals differed from those of normal animals. First, we did not observe unmyelinated fibers in either the vestibular nerve or the utricular macula of nerve-sectioned animals. Second, degenerated myelinated fibers were seen in large numbers in nerve-sectioned animals (arrows, Fig. 2b). These fibers, whose axolemmal diameters were distributed similarly to those of normal fibers (Fig. 2d), were assumed to be the degenerated remnants of vestibular efferent fibers (Robbins et al., '67; Dunn, '78; Gacek, '84).

The number and axolemmal diameter of myelinated fibers innervating the utricular macula, estimated by subtracting the number of ampullary nerve fibers from the number of fibers in the anterior vestibular nerve, are summarized in Table 1. In two normal animals, this calculation resulted in an estimate of $2,315 \pm 267$ myelinated fibers innervating the utricular macula. Similar calculations in two nerve-sectioned animals resulted in a total of $2,024 \pm 269$ myelinated fibers, of which $1,775 \pm 132$ were normal fibers and 249 ± 137 were degenerated fibers. Assuming that these degenerated myelinated fibers represent the remnants of vestibular efferent fibers, our analysis suggests that efferent neurons represent 10–15% of the normal utricular innervation.

Organization of the utricular macula

The utricular macula of the bullfrog is a kidney-shaped epithelium whose long and short axes, measured in eight dissected specimens, had mean values of 1.15 and 0.58 mm, respectively. The posterior part of the macula, as in mammals (Lindeman, '69; Wersall and Bagger-Sjoberg, '74; Fernandez et al., '90), lies in a nearly horizontal plane. Its anterior part is curved upwards. The utricular macula in the bullfrog is divided into a large medial zone and a smaller lateral zone by the striola, a 75–100 μm ribbon-shaped zone that runs for almost the entire length of the sensory epithelium near its lateral border (Fig. 1).

The plane of section is shown in Figure 1a and illustrated in Figure 1b. The cellular organization of the utricular macula is a pseudostratified columnar epithelium of sensory hair cells interspersed with nonsensory supporting

cells (Fig. 1b,c). Hair cells occupy the upper two-thirds of the sensory epithelium, while supporting cells span its entire distance. The nuclei of hair cells are positioned apical to those of supporting cells. The basal surfaces of supporting cells rest on or near a basement membrane that separates the sensory epithelium from its afferent and efferent innervation.

The striola differed in several respects from flanking extrastriolar regions. Hair cells in the striola tended to be larger in size and more widely spaced than hair cells located in the medial or lateral extrastriola (Fig. 1b). Hair cells in the utricular macula also differed markedly in their hair bundle morphology (Fig. 1b,c). In sectioned material, the apical surface of the striola was higher in elevation than the medial or lateral extrastriola, giving the striola a hill-like appearance (Figs. 1b, 3a,b). In either extrastriolar region, the orientation of hair cells was directed toward the striolar region. Hair cells within the striola were oriented in the same direction as adjacent extrastriolar cells. This orientation reversed within the striola, the line of reversal occurring lateral to the striolar midline. On average, the striola consisted of five to seven medial rows and two to three lateral rows of hair cells.

The boundaries between the striola and the medial and lateral extrastriola were easily recognized in both wholemount and sectioned material. Relative areas of these macular regions were determined in the four nerve-sectioned maculae that produced useful data. The striola made up $20.4 \pm 1.8\%$ of the sensory macula; the medial extrastriola, $64.7 \pm 2.5\%$; and the lateral extrastriola, $15.0 \pm 0.9\%$. Within the striola, the medial and lateral rows made up $16.3 \pm 2.2\%$ and $4.0 \pm 0.6\%$ of the macular area, respectively. To analyze regional variations in the utricular macula, a straight line was drawn across the endorgan to divide the striola and two extrastriolar regions into anterior and posterior halves (dashed line, Fig. 1). In the remainder of the paper, we shall refer to the anterior (SA) and posterior (SP) striola. The extrastriolar region is similarly divided into four quarters, designated as anterolateral (AL), anteromedial (AM), posterolateral (PL), and posteromedial (PM).

Peripheral innervation patterns

In nerve-sectioned animals, cell bodies and proximal axons in the vestibular nerve were, at best, only lightly labeled. The terminal axons and dendritic arbors of labeled afferents within the utricular macula, on the other hand, were darkly stained (Figs. 3a,b, 6a–f). The conclusions that follow are based on 333 labeled afferents obtained from the utricular maculae of four nerve-sectioned animals. Each labeled afferent was characterized by the diameter of its parent axon and the macular location at which it entered the sensory epithelium. The terminal fields of 144 afferents were sufficiently well isolated from other labeled fibers that they could be reconstructed in their entirety. For 56 of these afferents, we determined the number of synaptic endings and the number and type of hair cells innervated by the afferent fiber. We also qualitatively examined the terminal arbors of several dozen labeled afferents in four additional animals in which the vestibular nerve was not sectioned. This qualitative examination confirmed that the axon diameters, terminal fields, and synaptic morphology of labeled afferents were not obviously different in normal and nerve-sectioned animals, suggesting that cutting the cen-

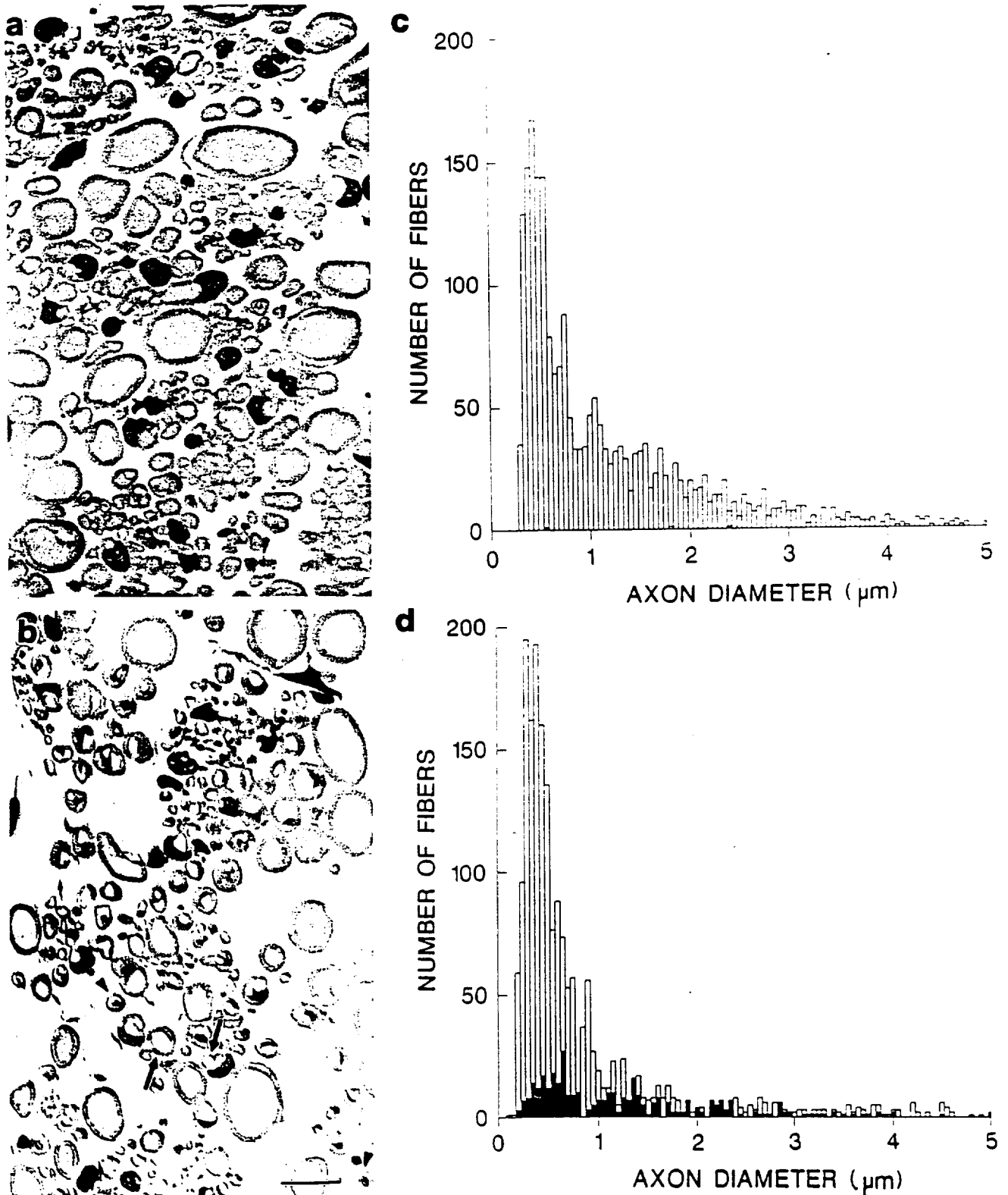


Fig. 2. Photomicrographs of Toluidine Blue-stained cross sections of the anterior vestibular nerve immediately medial to the utricular macula in a typical normal animal (a) and an animal sacrificed 14 days after sectioning of the eighth nerve medial to Scarpa's ganglion (b). Dark profiles in a and b represent the nuclei of Toluidine Blue-stained

Schwann cells. In b, arrows indicate representative degenerated axons lacking cytoplasmic material. Pointers indicate representative axons labeled with horseradish peroxidase. c,d: Histograms of axolemmal diameter of normal (open) and degenerated (solid) myelinated fibers in a normal (a) and a nerve-sectioned (b) animal. Bar = 10 μm.

TABLE 1. Counts of Myelinated, Degenerated, and Unmyelinated Fibers¹

Nerve branchlet	Normal animals				Nerve-sectioned animals		
	No.	Fiber type		No.	Fiber type		
		Normal	Degenerated		Normal	Degenerated	
AN	8,027	4012.0 ± 28.3	1.5 ± 0.7	7,598	3297.5 ± 87.0	501.5 ± 212.8	
HC	1,787	803.5 ± 145.0	0	1,768	735.0 ± 132.9	149.0 ± 76.4	
AVC	1,627	813.5 ± 94.0	0	1,782	787.5 ± 88.4	103.5 ± 0.7	
UN	4,633	2315.0 ± 267.3	1.5 ± 0.7	4,048	1775.0 ± 131.5	249.0 ± 137.2	

¹Values are means ± SD; No., total number of axon profiles from two normal animals and two nerve-sectioned animals. Axon diameters are corrected for differential shrinkage (see Materials and Methods). Axon profiles are obtained from the anterior nerve (AN), horizontal semicircular canal (HC), and anterior vertical semicircular canal (AVC). Values for the utricular branchlet (UN) are estimated from the formula UN = AN - HC - AVC.

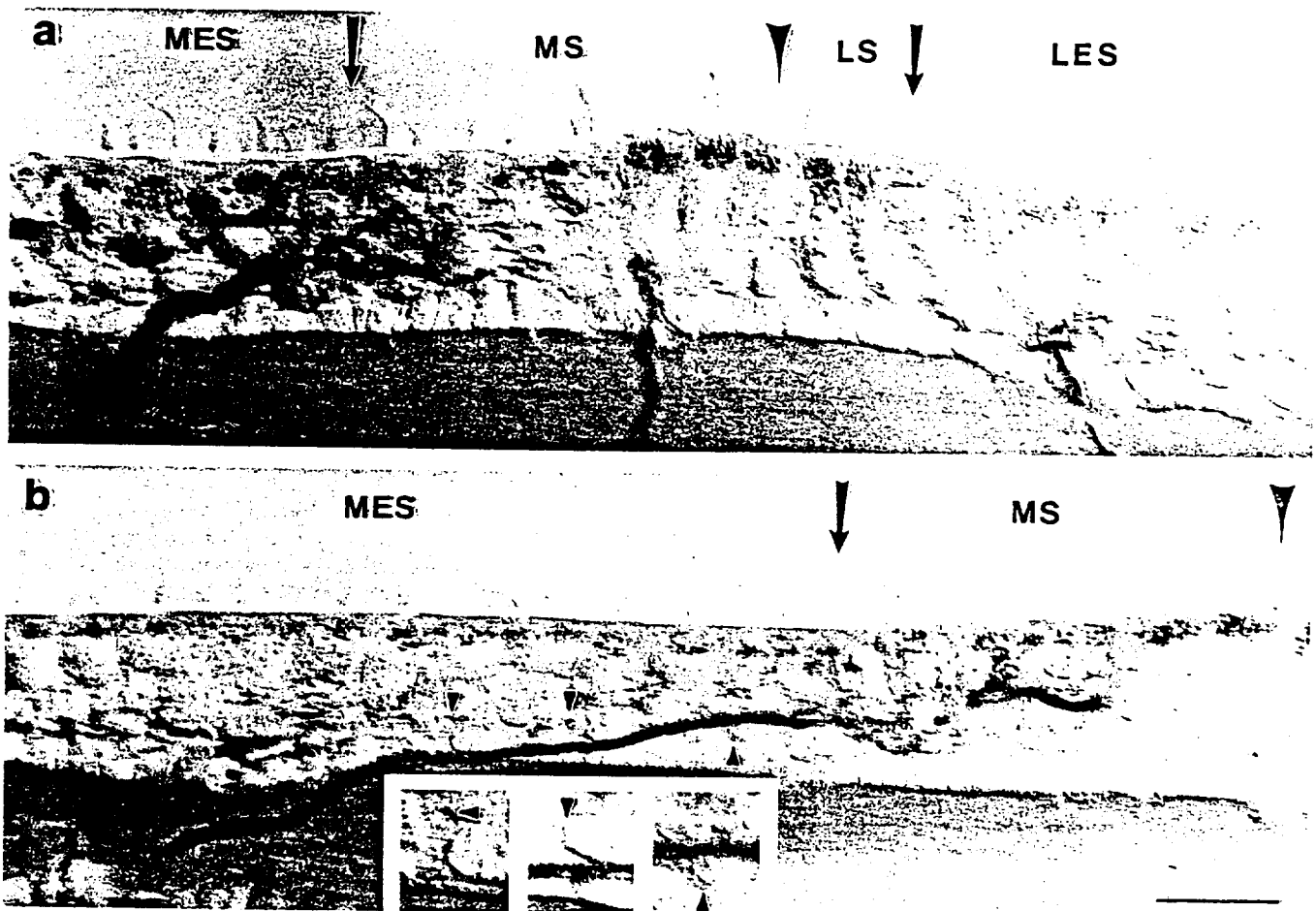


Fig. 3. Photomicrographs of the cross-sectioned striola (a) and medial extrastriola (b) of the utricular macula. The small dark particles near the apical surfaces of hair cells are peroxidase-containing organelles (probably mitochondria) labeled by the histological procedure used to visualize horseradish peroxidase. Three horseradish peroxidase-labeled afferents, located in the medial striola (left), central striola (middle), and lateral extrastriola (right) are seen in a. In b, one branch of a bifurcating juxtastriolar afferent is seen. Small collateral branches,

indicated by small arrowheads in the main figure and in the insets below, terminate in bouton-like endings. A second horseradish peroxidase-labeled afferent (right), located in the medial striola, is also seen. In a, arrows denote the medial (left) and lateral (right) striolar borders; in b, a single arrow indicates the medial striolar border. Large arrowhead indicates the reversal of hair cell polarization. MES, medial extrastriola; MS, medial striola; LS, lateral striola; LES, lateral extrastriola. Bars = 250 μm in a, 25 μm in b.

tral processes of vestibular afferents did not alter the normal morphology of their peripheral processes.

The utricular nerve branchlet separates from the anterior branch of the vestibular nerve. As in mammals (Fernandez et al., '90), some fibers run immediately under the connective tissue stroma and pass through it to reach the curved anterior portion of the macula. Afferent fibers supplying more posterior regions first entered a fiber layer

located at the bottom of the stroma. The latter fibers, upon reaching their destinations, bend sharply upwards and take a direct course through the stroma and into the sensory epithelium. Fibers supplying the lateral macula often run past the edge of the macula before returning medially and bending sharply upwards through the sensory epithelium.

A small (43/333 = 12.9%) proportion of utricular afferents bifurcated below the sensory epithelium, typically

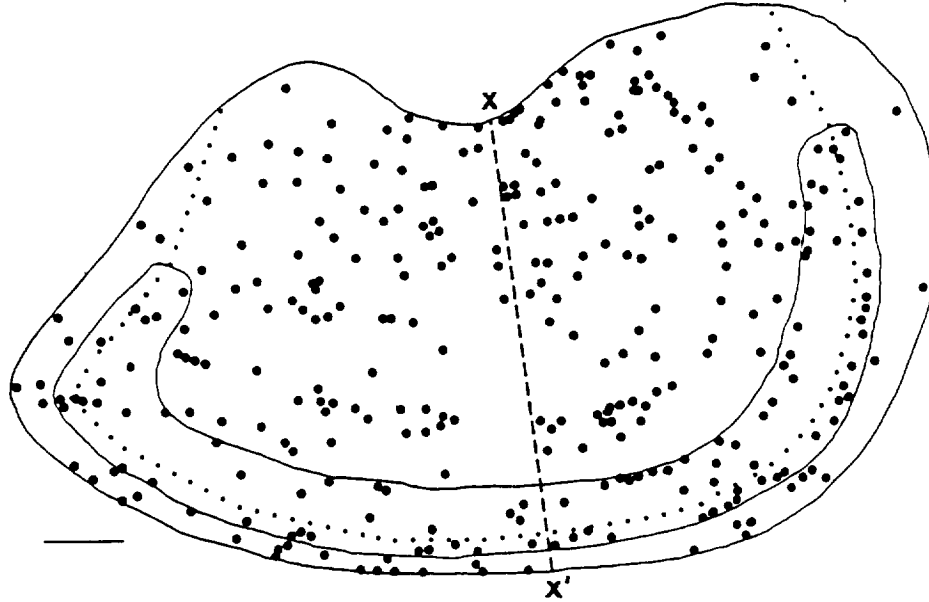


Fig. 4. Distribution of 92 striolar and 241 extrastriolar afferents indicated on a standard surface map of the utricular macula. The striola, a thin ribbon-shaped area, and its anterior and posterior

extensions (dotted lines) separate the extrastriola into a larger medial and a smaller lateral zone. A dashed line (x---x') divides the macula into anterior and posterior halves. Bar = 100 μ m.

within 10–30 μ m of the basement membrane. Bifurcations were found in axons destined for both the striolar (9/92 = 9.8%) and extrastriolar (34/241 = 14.1%) regions. More than three-quarters of these fibers had single branch points (Figs. 7b, 8a). In a few units, one or both primary branches divided a second time (Fig. 7a). The branches of bifurcating afferents were usually similar in diameter and innervated contiguous or closely adjacent groups of hair cells in the same part of the sensory epithelium.

The branches of bifurcating fibers as well as the parent axons of nonbifurcating fibers typically began dividing into their terminal arborizations within 10–20 μ m after crossing the basement membrane. Some axons in the medial extrastriola were exceptional in this regard. For these fibers, the axon ran unbranched in the lower part of the epithelium without giving rise to synaptic endings (right branch, Fig. 8a) or giving rise to only a small number of thin collateral branches (insets, Fig. 3b; left branch, Fig. 8a,b–d) for up to 50 μ m before dividing into their terminal arborizations. The arborizations of utricular afferents were compact, seldom extending more than 50–75 μ m in any direction from the parent axon.

Utriclar afferents were classified as striolar or extrastriolar according to the epithelial entrance of their parent axons and the macular location of their terminal fields. The parent axons of two striolar afferents, one innervating the outer rows (left) and one supplying the inner rows (middle) of the medial striola, are shown in Figure 3a. A third afferent, innervating the lateral extrastriola, is shown to the far right. The epithelial entrances of all 333 labeled afferents are indicated with dots on a standard surface map of the utricular macula in Figure 4. In this figure, the striola, a thin ribbon-shaped area, and its anterior and posterior extensions (dotted lines) separate the extrastriolar region into a larger medial and a smaller lateral zone. A dashed line (x---x') divides the macula into anterior and posterior halves.

The percentages of afferents in the anterior and posterior striola and in the four quarters of the extrastriola are shown in Table 2. The proportions are close to those expected on an areal basis. Thus, the division of afferents between the striola (27.6%) and the extrastriola (72.4%) is similar to the 20.4–79.6% split expected from the relative areas of these two zones. The major discrepancy is the presence of a larger number of afferents in the anterior striola than would be expected on an areal basis (16.2% vs. 10.2%, respectively). With two exceptions, the proportion of afferents in the extrastriola also parallels the relative areas of the four extrastriolar zones: 1) there were slightly more afferents in the anteromedial region than in the posteromedial region; and 2) there were fewer afferents in the anterolateral region than expected on an areal basis.

Table 2 also compares the morphological characteristics of striolar and extrastriolar afferents innervating different regions of the utricular macula. The legend to Table 2 summarizes the results of statistical tests. When striolar and extrastriolar afferents are compared, the former have thicker parent axons, fewer subepithelial bifurcations, and larger terminal fields than the latter. There were also regional differences among both striolar and extrastriolar afferents. Afferents in the posterior striola had more frequent subepithelial bifurcations and larger terminal fields than afferents in the anterior striola. Among extrastriolar afferents, afferents in the lateral zone had larger parent axons and larger terminal fields than afferents in the medial zone. Afferents in the anterolateral extrastriola also had more frequent subepithelial bifurcations than afferents in other extrastriolar regions. Other regional differences among striolar and extrastriolar afferents were small and statistically insignificant.

Afferents in a juxtastricular zone, immediately adjacent to the medial striola, had innervation patterns that were transitional between those in the striola and more peripheral parts of the medial extrastriola. Afferents supplying

TABLE 2. Regional Characteristics of Labeled Afferents¹

Fiber type	All fibers				Reconstructed fibers				
	No.	Percent (%)	Axon (μm)	Bifurcations (%)	No.	Long axis (μm)	Short axis (μm)	Terminal area (μm ²) (C _T)	
Striola	92	27.6	2.17 ± 0.92	9.8	35	64.2 ± 17.4	38.2 ± 9.7	1,383 = 550	
SA	54	16.2	2.18 ± 0.94	0	21	61.5 ± 18.3	35.6 ± 7.5	1,124 = 304	
SP	38	11.4	2.16 ± 0.88	23.7	14	68.9 ± 14.0	42.4 ± 10.9	1,771 = 588	
Extrastriola	241	72.4	1.06 ± 0.52	14.1	107	46.8 ± 23.0	26.2 ± 12.3	746 = 594	
AM	105	31.5	0.98 ± 0.43	11.4	54	42.3 ± 19.2	24.6 ± 12.7	634 = 563	
PM	93	27.9	0.96 ± 0.46	15.0	43	45.5 ± 18.9	26.9 ± 12.1	747 = 566	
AL	14	4.2	1.32 ± 0.57	28.6	2	62.8 ± 9.2	42.8 ± 5.2	1,544 = 291	
PL	29	8.7	1.52 ± 0.68	13.8	8	80.2 ± 38.8	28.6 ± 8.4	1,346 = 532	

¹Values are means ± SD; No., number of afferents. Percent of total is percentage of all labeled afferents. Axon diameters are corrected for differential shrinkage (see Materials and Methods). Bifurcations (%) is the percentage of axons in each category that branched below the basement membrane. Terminal-field areas are expressed in μm² and as a percentage of macular surface area. Striolar afferents supply the anterior (SA) or posterior (SP) striola. Extrastriolar afferents supply the anteromedial (AM), anterolateral (AL), posteromedial (PM), or posterolateral (PL) macula. The following differences were statistically significant. Axon diameter: SA + SP vs. AM + PM, SA vs. AL + PL, P < 0.0001 in all cases; SP vs. AL, P < 0.0005; SP vs. PL, PL vs. AM + PM, P < 0.001 in all cases. Long axis: PL vs. AM + PM, P < 0.0001 in all cases; SP vs. AM, P < 0.0005; SA vs. AM, SP vs. PM, P < 0.005; SA vs. PM, P < 0.05. Short axis: SP vs. AM, P < 0.0001; SP vs. PM, P < 0.0005; SA vs. AM, P < 0.005; SA vs. PM, P < 0.05. Terminal area: SP vs. AM + PM, P < 0.0001 in all cases; SA vs. AM, P < 0.005; SP vs. SA, PL vs. AM, P, 0.01; PL vs. PM, P < 0.05.

TABLE 3. Zonal Characteristics of Labeled Afferents¹

Fiber type	All fibers				Reconstructed fibers				
	No.	Percent (%)	Axon (μm)	Bifurcations (%)	No.	Long axis (μm)	Short axis (μm)	Terminal area (μm ²) (C _T)	
Striola	92	27.6	2.17 ± 0.92	9.8	35	64.2 ± 17.4	38.2 ± 9.7	1,383 = 550	
MS	51	15.3	2.15 ± 0.93	5.9	26	63.8 ± 19.9	39.4 ± 10.0	1,423 = 605	
LS	41	12.3	2.20 ± 0.93	14.6	9	65.9 ± 9.5	34.8 ± 8.5	1,267 = 349	
Juxtastriola	65	19.5	1.35 ± 0.51	7.7	17	67.2 ± 13.1	42.6 ± 12.1	1,505 = 620	
Extrastriola	17	52.8	0.95 ± 0.48	16.5	92	42.3 ± 23.3	23.5 ± 10.1	609 = 476	
MES	13	39.9	0.79 ± 0.25	15.8	82	39.4 ± 16.9	22.5 ± 9.8	516 = 383	
LES	43	12.9	1.45 ± 0.64	18.6	10	76.8 ± 35.1	31.4 ± 9.7	1,386 = 486	

¹Values are means ± SD; No., number of afferents. Percent of total is percentage of all labeled afferents. Axon diameters are corrected for differential shrinkage (see Materials and Methods). Bifurcations (%) is the percentage of axons in each category that branched below the basement membrane. Terminal areas are expressed in μm² and as a percentage of macular surface area. Striolar afferents supply the medial (MS) or lateral (LS) striola; extrastriolar afferents supply the medial (MES) or lateral (LES) extrastriola. The following differences were statistically significant. Axon diameter: juxtastriola + LES vs. LS + MS + MES; LS + MS vs. MES, P < 0.0001 in all cases. Long axis: juxtastriola + MS vs. MES, P < 0.0001 in all cases; LS vs. MES, P < 0.0005. Short axis: juxtastriola + MS vs. MES, P < 0.0001 in all cases; LS vs. MES, P < 0.005; juxtastriola vs. LES, P < 0.05. Terminal area: LS + LES + juxtastriola vs. MES; MS vs. MES, P < 0.0001 in all cases.

this zone tended to enter the sensory epithelium approximately 100 μm from the medial striolar border (Fig. 4). They then traveled laterally perpendicular to the striola giving rise to few, if any, synaptic endings for relatively long distances (Figs. 3b, 8a-d). Relatively few afferents entered the sensory epithelium within 100-200 μm of the medial striolar border (Fig. 4).

The morphological characteristics of striolar, juxtastriolar, and extrastriolar afferents are compared in Table 3. The legend to Table 3 also summarizes the results of statistical tests. Juxtastriolar afferents resembled striolar afferents, tending to have thicker parent axons, fewer subepithelial bifurcations, and larger terminal fields than afferents supplying more peripheral regions of the medial extrastriola. There were also regional differences between afferents supplying the medial and lateral extrastriolar zones. Afferents in the lateral extrastriola, for example, had larger parent axons and larger terminal fields than afferents in the medial extrastriola. By contrast, afferents in the lateral striola had more frequent subepithelial bifurcations and smaller terminal fields than afferents in the medial striola. The morphological characteristics of juxtastriolar afferents closely resembled those of lateral extrastriolar afferents, suggesting that many of the properties of utricular afferents were a function of their relative proximity to the striolar region.

Striolar, juxtastriolar, and extrastriolar afferents also differed in the size and orientation of their terminal fields. This can best be appreciated from Figure 5a, which illustrates the terminal fields of 33 fully reconstructed afferents.

The long and short axes of terminal fields in the peripheral margins of the medial extrastriola were short and similar in size. These fields were small, representing on average 0.09% of the total macular area. The terminal fields of medial extrastriolar afferents closer to the striolar region were larger and more elongate. In the juxtastriola, for example, the long axes of terminal fields were significantly larger than their short axes, increasing their area on average to 0.27% of the total macular area. The long axes of these afferents were oriented parallel to the direction of hair cell morphological polarization, which was generally perpendicular to the striolar border (Fig. 5b). In contrast, terminal fields within the striola were largely oriented parallel to the striolar border, at right angles to the direction of hair cell morphological polarization. This was particularly true of afferents supplying the central and lateral striola and was also true of afferents supplying the lateral extrastriolar region. On average, terminal fields in the striola and lateral extrastriola represented 0.25% of the total macular area.

Labeled afferents in the utricular macula possessed several types of specialized endings. These endings, which were observed in close proximity to hair cells, may represent points of synaptic contact between hair cells and utricular nerve afferents. Afferents in both the striolar and extrastriolar regions commonly possessed dendritic swellings that resembled en passant (left arrow, Fig. 6a) and terminal (right arrow, Fig. 6a; arrows, Fig. 6b) bouton endings. The size and shape of these endings varied considerably. The smallest endings were round, with diameters of 0.5 μm

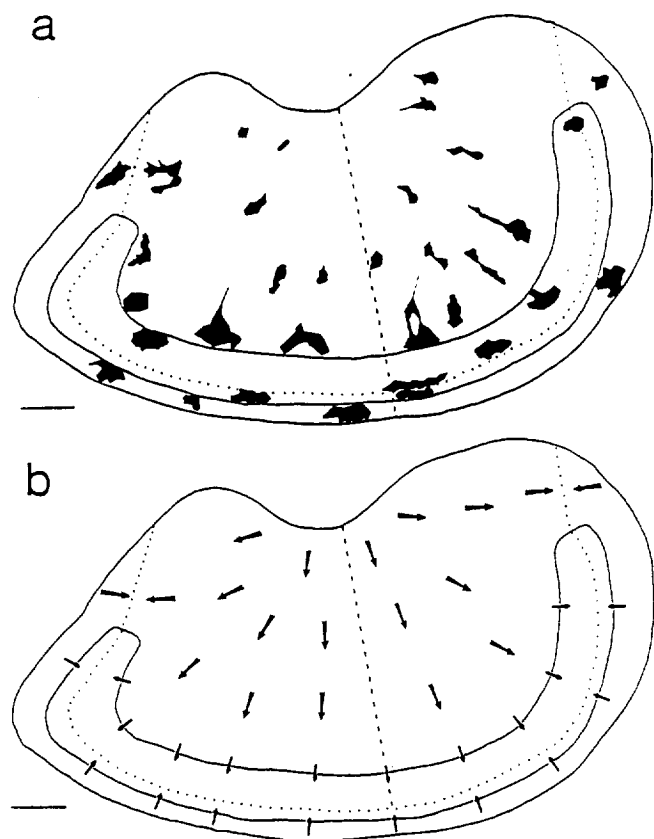


Fig. 5. a: Orientation of the terminal arbors of 7 striolar and 26 extrastriolar afferents indicated on a standard surface map of the utricular macula. b: Map of hair cell morphological polarization (adapted from Lewis and Li, '75). The striola, a thin ribbon-shaped area, and its anterior and posterior extensions (dotted lines) separate the extrastriola into a larger medial and a smaller lateral zone. A dashed line (x--x') divides the macula into anterior and posterior halves. Bars = 100 μ m.

(arrows, Fig. 6a). Larger endings were ovoid in appearance, with widths and lengths up to 3 μ m and 5 μ m, respectively (arrows, Fig. 6b). Bouton-like endings were also infrequently observed in close proximity to the basement membrane, suggesting that they might be contacting the cell bodies of supporting cells (compare Figs. 1b and 6c). Bouton-like endings, whether en passant or terminal, were typically located on thin branches <1 μ m in diameter. Other labeled afferents, especially in the striolar region, possessed other types of specialized endings. These included club endings, large (2–3 μ m) rounded terminals (arrow, Fig. 6d), and fine (<0.5 μ m) dendritic spines (arrow, Fig. 6e), both of which emerged directly from thick dendritic branches. Hair cells in both striolar and extrastriolar regions were also contacted by claw-like endings that partially enveloped their basolateral surfaces (arrow, Fig. 6f). The branching patterns and synaptic morphology of striolar, juxtastriolar, and extrastriolar afferents differed and will be described separately.

Extrastriolar afferents

There were 80 fully reconstructed afferents in the medial extrastriola. These afferents had thin (<1 μ m) parent axons, which, upon entering the sensory epithelium, rap-

idly bifurcated into numerous smaller branches. These branches arose as collaterals from the parent axon (Fig. 7a,b,d–f) or one of its thick branches (Fig. 7b,f). Arborizations were compact, seldom extending >50 μ m in any direction from the parent axon. Medial extrastriolar afferents varied in complexity from those with <15 bouton-like endings (Fig. 7d,e) to those with >50 bouton-like endings (Fig. 7b). These endings varied tremendously in size (Fig. 6a,b).

Afferents supplying the peripheral margin of the medial extrastriola differed in several respects from afferents innervating more central portions of the medial extrastriola. Unlike more centrally located afferents, afferents on the medial margin had thinner parent axons, more subepithelial bifurcations, and larger numbers of apparent synaptic endings. Afferents supplying the peripheral margin also appeared to contact cells without hair bundles located outside the sensory macula and hair cells with immature hair bundles located on the macular border (Fig. 7a). Marginal afferents, unlike other medial extrastriolar afferents, often contacted hair cells with large claw-like endings (arrow, Fig. 6f; asterisk, Fig. 7a).

The terminal arbors of ten fully reconstructed afferents in the lateral extrastriola were significantly larger than those of medial extrastriolar afferents. These arbors arose from thicker parent axons than those of medial extrastriolar afferents and branched profusely, producing >150 bouton-like endings (Fig. 7c,g). The bouton-like endings of afferents in the lateral extrastriola, unlike those of medial extrastriolar afferents, were uniformly small (Fig. 6a). More specialized types of endings were not observed in lateral extrastriolar afferents.

The terminal fields of lateral extrastriolar afferents were usually confined to the extrastriolar zone (right, Fig. 3a). A typical example of such an afferent, which extends medially but stays within the lateral extrastriola, is shown in Figure 7g. Only three of ten lateral extrastriolar afferents were observed to cross the lateral striolar border. None of these afferents had similar numbers of endings or contacted similar numbers of hair cells in the striolar and extrastriolar zones. Rather, they typically extended a single branch or a small number of branches over the striolar border, contacting one to four striolar hair cells (Fig. 7c).

Juxtastriolar afferents

There were 17 afferents assigned to the juxtastriolar region. Juxtastriolar afferents typically had medium-sized parent axons that entered the sensory epithelium medial to the striola and ran laterally in the lower part of the sensory epithelium for 25–50 μ m, giving rise to few, if any, apparent synaptic endings (insets, Fig. 3b). In a few cases, the parent axons of juxtastriolar afferents were bifurcated, both branches running laterally in the lower part of the sensory epithelium (Fig. 8a). They then intermittently gave rise to small collateral branches that contacted single hair cells or small clusters of hair cells (Fig. 8b–d) with bouton-like endings. At their most lateral extent, the parent axons of juxtastriolar afferents bifurcated into numerous smaller branches that terminated in bouton-like endings (Fig. 8a–d). The terminal arbors of juxtastriolar afferents were the largest in the utricular macula, often extending laterally >100 μ m from their entrance into the sensory epithelium. These afferents typically had >150 bouton-like endings, which, with few exceptions (Fig. 8b), were uniformly small in size. Juxtastriolar afferents that terminated near

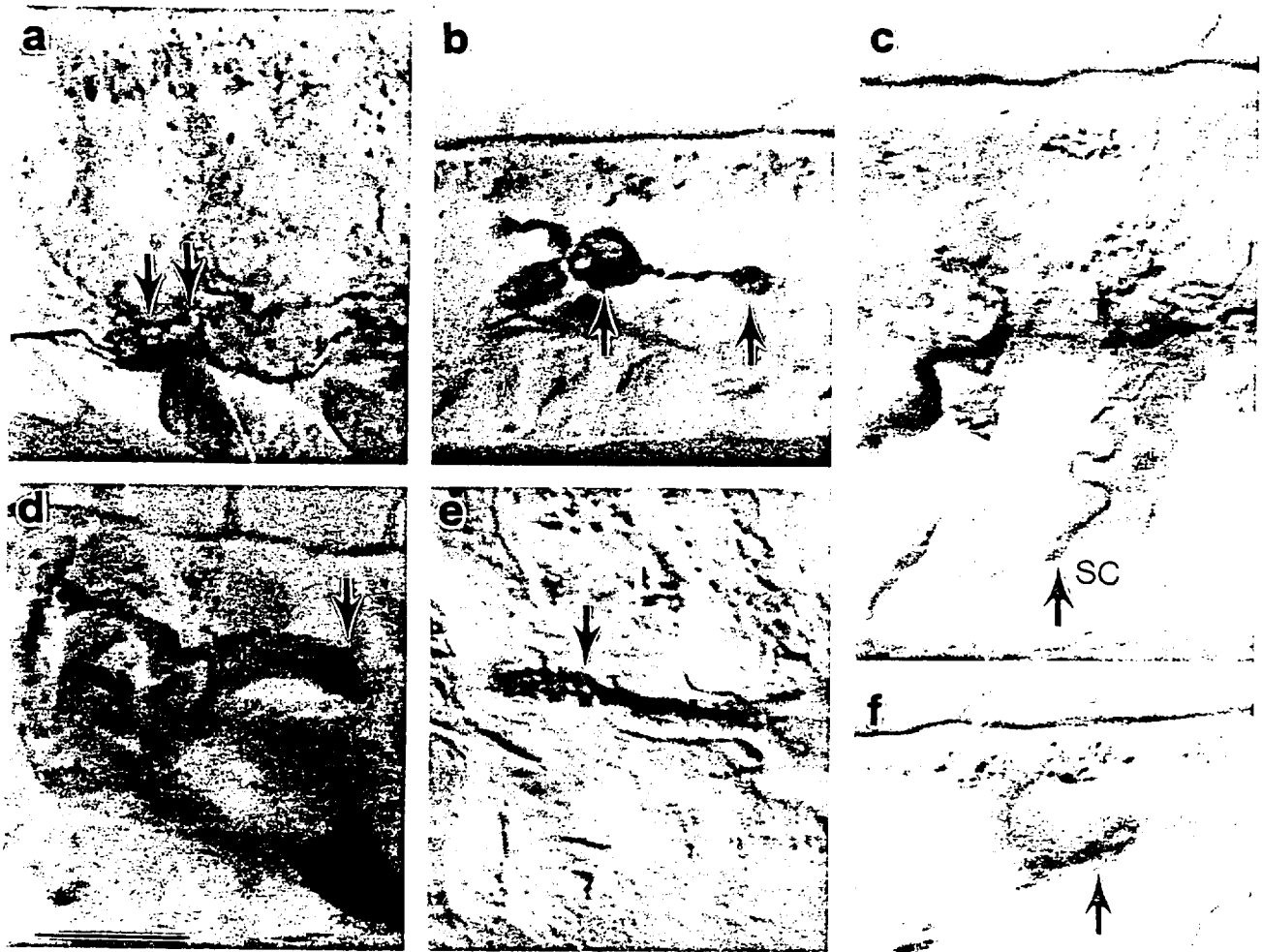


Fig. 6. a,b: Photomicrographs of small (a) and large (b) bouton-like endings in afferents labeled by horseradish peroxidase. Arrows indicate en passant (left) and terminal (right) bouton-like endings. c: Photomicrograph of a terminal bouton-like ending contacting a cell located immediately adjacent to the basement membrane, suggesting that

supporting cells (SC) as well as hair cells are innervated by vestibular afferents. d-f: Photomicrographs of other putative synaptic endings, including club endings (d), dendritic spines (e), and claw-like synaptic endings (f). In each case, arrows mark the location of the appropriate ending. Bar = 10 μ m.

the striola border (Fig. 8a,b,d) tended to have more extensive arbors than those located further away (Fig. 8c).

The terminal fields of juxtastricular afferents were usually confined to the medial extrastricular. Of 7/17 (41.2%) afferents that crossed the striolar border, none had similar numbers of synaptic endings or was contacted by similar numbers of hair cells in the two zones. Rather, they typically extended a single branch or a few branches over the striolar border, innervating from two to ten striolar hair cells (Fig. 8a,b). On average, this represented 10.3% of the total innervation of these afferents. A more extreme situation is illustrated in Figure 8d, in which a juxtastricular afferent that straddled the striolar region extended into the middle striolar rows, innervating 20 striolar hair cells.

Striolar afferents

Within the striolar region, 32 afferents, including 24 in the medial and 8 in the lateral striola, were fully reconstructed. Striolar afferents typically had thick (>2 μ m) parent axons that did not bifurcate below the sensory epithelium (left, Fig. 3a). Many (16/32) of these afferents

entered the sensory epithelium within 10–20 μ m of the medial (Fig. 9a–d) or lateral (Fig. 9g) striolar border. Other striolar afferents (10/32), particularly in the medial striola, entered the sensory epithelium somewhat more centrally (Fig. 9e). In both cases, the parent axons of these afferents began bifurcating immediately into many large collateral branches, tapering in diameter and dividing into numerous smaller processes. A small (6/32) number of striolar afferents with thin parent axons innervated the innermost rows of the striolar region (middle, Fig. 3a). These axons, upon entering the sensory epithelium, ran anteriorly and/or posteriorly for long distances, intermittently giving rise to short, thin collateral branches that contacted small clusters of hair cells with bouton-like endings (Fig. 9f). These afferents, unlike other striolar afferents, had long, narrow terminal fields oriented parallel to the striolar border.

Striolar afferents varied in complexity from those with <100 endings (Fig. 9c) to those with >350 endings (Fig. 9e). As in other macular regions, striolar afferents largely contacted hair cells with bouton-like endings. In addition, striolar afferents possessed club endings, large (2–3 μ m)

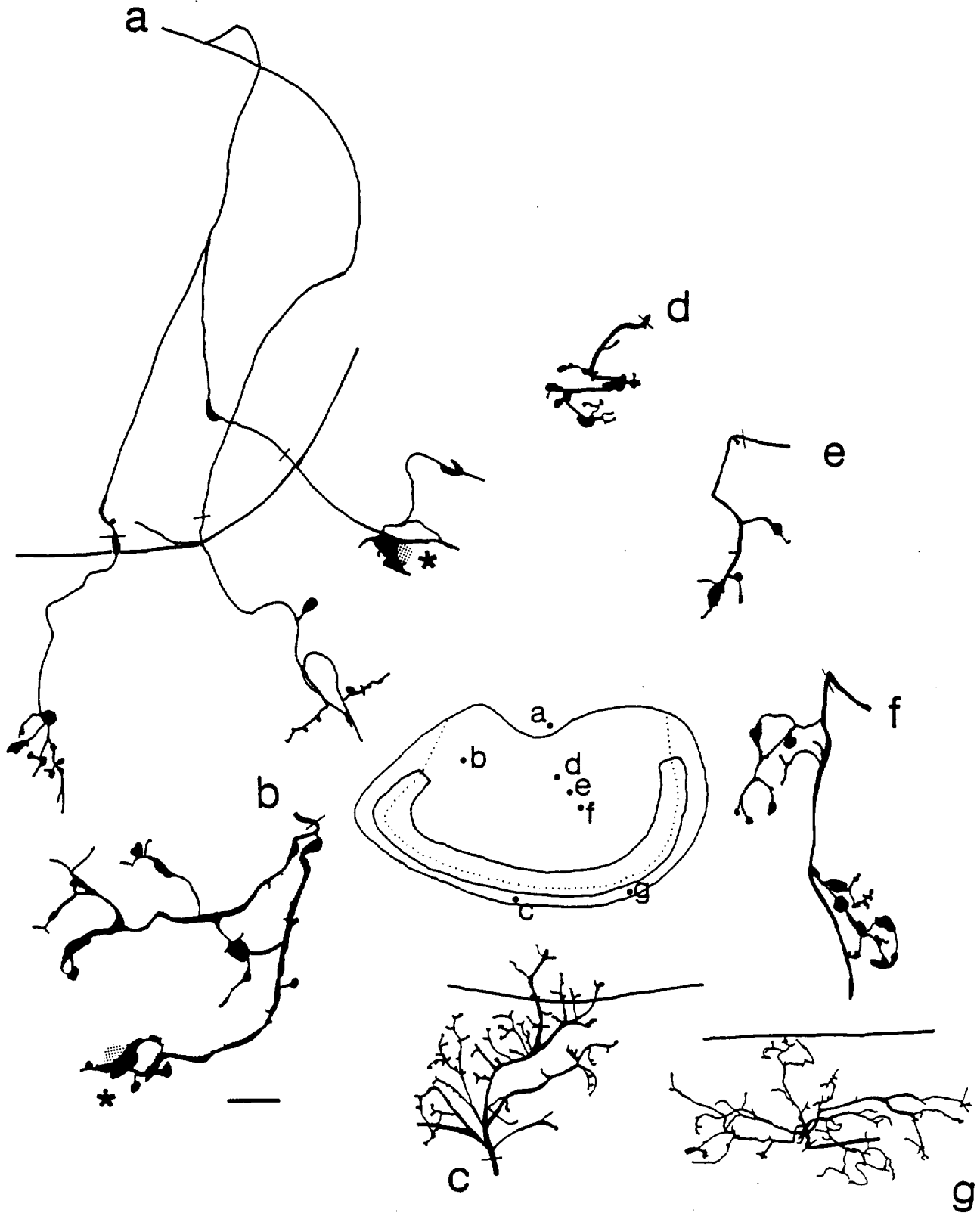


Fig. 7. Reconstructions of seven afferents located in the medial (a, b, d-f) and lateral (c, g) extrastriola, with macular locations indicated on a standard surface map of the utricle (inset). In this and following figures, thin line segments in each drawing indicate the entrance point of the parent axon or its bifurcating branch(es) into the

sensory epithelium. In a and b, asterisks indicate claw-like endings that partially surround the basal surface of innervated hair cells. Solid line in a indicates the macular border; similar lines in f and g indicate the lateral striolar border. Bar = 10 μ m.

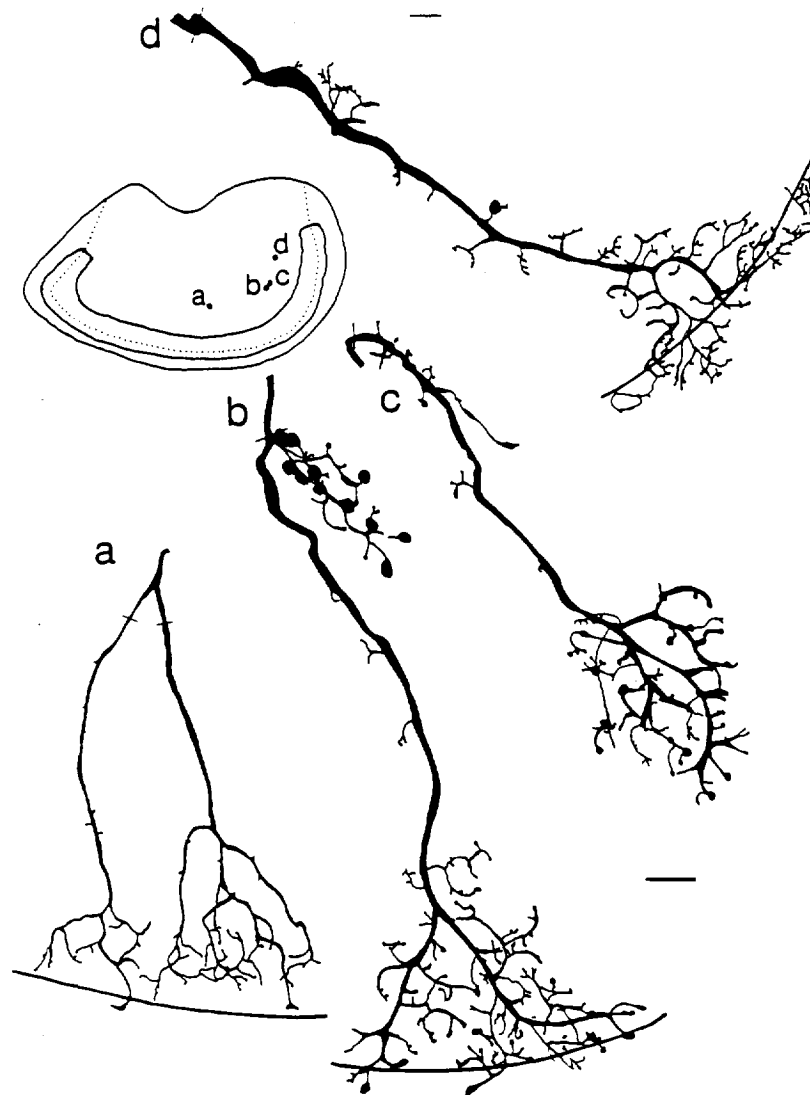


Fig. 8. Reconstructions of four afferents located in the juxtastriola (a-d), with macular locations indicated on a standard surface map of the utricular macula (inset). Thin line segments in each drawing indicate the entrance point of the parent axon or its bifurcating branch(es) into the sensory epithelium. Solid lines in selected drawings indicate the medial striolar border. Bar = 10 μ m.

rounded terminals that emanated directly from thick dendritic branches to contact single hair cells (Figs. 6e, 9g). Striolar afferents were also observed to contact hair cells with dendritic spines, small (<0.5 μ m) endings that, like club endings, emerged directly from thick dendritic processes (Figs. 6e, 9e).

The terminal fields of striolar afferents were relatively compact in two respects. First, they were generally confined to the medial or lateral side of the striolar region. This was true of 19/24 afferents in the medial striola and 3/8 afferents in the lateral striola. Striolar afferents with thick (>2 μ m) parent axons were also more likely to have terminal fields restricted to one side of the striolar region than striolar afferents with thin (<2 μ m) parent axons, regardless of whether they entered the sensory epithelium in the outer or inner striolar rows. The terminal fields of 20/26 striolar afferents with thick parent axons, for example, were confined to either the medial or lateral side of

the striolar region. An example of a medial striolar afferent, which extended laterally but stayed within the medial striola, is shown in Figure 9e. Of the six remaining striolar afferents with thick parent axons, none had similar numbers of endings or contacted similar numbers of hair cells in the medial and lateral striola. Rather, they typically extended a single branch over the striolar border, contacting one to four hair cells in the opposing striolar region. One such afferent, originating in the lateral striola, is shown in Figure 9g. A majority (4/6) of striolar afferents with thin parent axons, on the other hand, often encompassed both sides of the striolar region (Figs. 9f, 10d). It was not uncommon for these afferents to have similar numbers of synaptic endings or to contact similar numbers of hair cells on the two sides of the striolar zone. This organization has a functional implication. Since hair cells in the medial and lateral parts of the striola have opposed morphological polarizations (Lindeman, '69; Wersall and Bagger-Sjoberg,

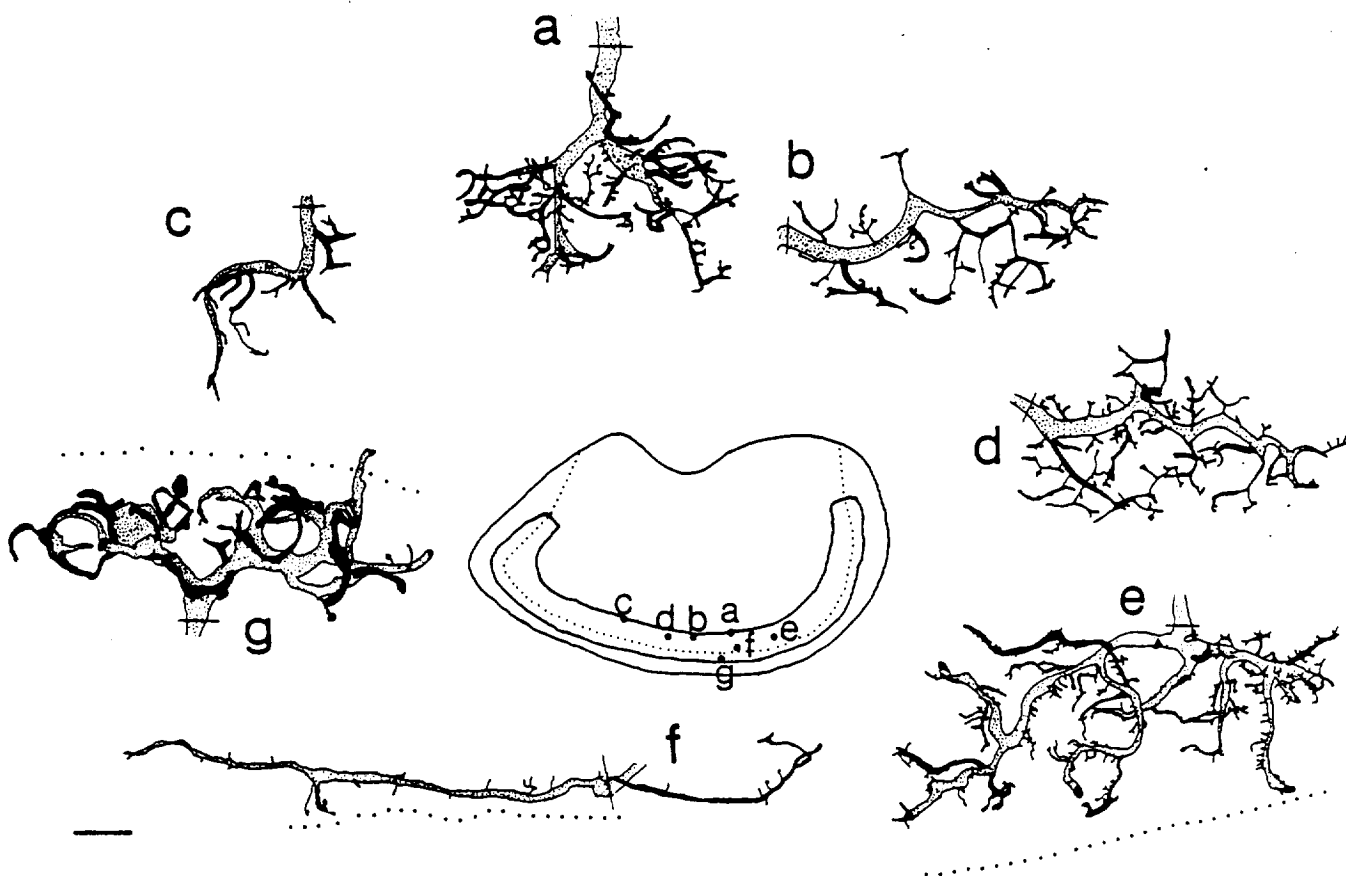


Fig. 9. Reconstructions of seven afferents located in the medial (a-e), central (f), and lateral (g) striola, with macular locations indicated on a standard surface map of the utricular macula (inset). The parent axons and larger collateral branches of afferents have been stippled and the thinner collateral branches blackened for graphical

clarity. Thin line segments in each drawing indicate the entrance point of the parent axon or its bifurcating branch(es) into the sensory epithelium. Dotted lines in selected drawings indicate the reversal of hair cell polarization. Bar = 10 μ m.

'74), restricting their terminal fields to one side of the striolar region ensures that an afferent will only contact hair cells with similar directional properties.

Second, the terminal fields of striolar afferents did not extend beyond the medial or lateral striolar border. This was true of 19/24 afferents in the medial striola and 7/8 afferents in the lateral striola. This arrangement suggests that the innervation of the striolar and the extrastriolar regions is relatively independent. This is confirmed by the observation that 43/56 reconstructed afferents (26/32 striolar, 10/17 juxtastriolar, and 7/10 lateral extrastriolar) were restricted to their zones of origin. No juxtastriolar or lateral extrastriolar afferent that crossed the striolar border had similar numbers of synaptic endings or contacted similar numbers of hair cells in the striolar and extrastriolar zones.

Synaptic endings and hair cell types

The numbers of synaptic endings and hair cells supplied by 139 reconstructed afferents are compared in Table 4. The legend to Table 4 also summarizes the results of statistical tests. Among 39 extrastriolar and juxtastriolar afferents on which synaptic counts were performed, it was observed that an individual hair cell could receive from one to four synaptic endings from a given afferent. This resulted in an average number of 1.9 ± 0.7 synaptic endings/

hair cell. This ratio rose sharply to 5.0 ± 1.6 for 17 afferents in the striolar region, where individual hair cells could receive as many as 15 synaptic endings. The average number of synaptic endings per hair cell in striolar afferents with thick parent axons was similar for all hair cell types. In striolar afferents with thin parent axons, Type B hair cells received significantly fewer synaptic contacts than other hair cell types.

Afferents in the medial extrastriola were the only afferents to innervate uniformly a single hair cell type, contacting 15.4 ± 10.6 Type B hair cells (Table 4). Juxtastriolar and lateral extrastriolar afferents, with the exception of ten afferents that supplied both the striolar and extrastriolar zones, also exclusively innervated Type B hair cells. The mean number of Type B hair cells contacted by medial extrastriolar afferents was significantly lower than that contacted by juxtastriolar or lateral extrastriolar afferents. Juxtastriolar and lateral extrastriolar afferents contacted similar numbers of Type B hair cells, lending further support to the suggestion that the morphological characteristics of utricular afferents were largely determined by their proximity to the striolar region.

The distribution of hair cell types innervated by a striolar afferent was a function of the macular entrance of its parent axon. The distribution of hair cell types contacted by

TABLE 4. Hair Cells, Synaptic Endings, and Afferent Nerve Fibers¹

Fiber type	No.	Number of hair cells					Total n _T	No.	Synaptic endings n _S	Endings hair cell n _S n _T
		Type B n _B	Type C n _C	Type F n _F	Type E n _E					
Striola	32	11.9 ± 7.0	21.9 ± 11.9	3.0 ± 3.3	5.3 ± 6.3	42.1 ± 14.5	17	178.9 ± 72.0	5.02 ± 1.60	
MS	24	13.1 ± 7.6	20.0 ± 10.6	2.7 ± 3.4	4.3 ± 6.4	40.1 ± 12.7	14	184.1 ± 78.7	5.02 ± 1.75	
LS	8	8.1 ± 2.1	27.6 ± 14.5	3.9 ± 3.1	8.3 ± 5.1	47.9 ± 18.6	3	154.7 ± 11.6	4.98 ± 0.76	
Juxtastriola	17	57.6 ± 22.1	3.1 ± 4.9	0.3 ± 0.8	0	61.4 ± 21.8	5	128.4 ± 37.9	1.82 ± 0.36	
Extrastriola	90	21.1 ± 20.9	0.1 ± 0.4	0	0	21.2 ± 21.1	34	29.2 ± 31.9	2.09 ± 0.87	
MES	80	15.4 ± 10.6	0	0	0	15.4 ± 10.6	32	23.0 ± 13.5	2.07 ± 0.86	
LES	10	67.0 ± 26.7	0.6 ± 1.3	0	0	67.6 ± 26.6	2	138.5 ± 71.4	2.38 ± 1.32	

¹Values are means ± SD; No., number of afferents. Table indicates number of synaptic endings (n_S) and the number of Type B (n_B), Type C (n_C), Type E (n_E), Type F (n_F), and total number (n_T) of hair cells innervated by afferents in each category. The following differences were statistically significant. Type B cells: LES vs. MES + MS + LS; juxtastriola vs. MES + MS + LS, P < 0.0001 in all cases. Type C cells: LS vs. MES; MS vs. juxtastriola + LES; LS vs. juxtastriola + LES, P < 0.0001 in all cases. Type F cells: LS vs. juxtastriola + MES + LES; MS vs. juxtastriola + MES + LES, P < 0.0001 in all cases. Type E cells: LS vs. juxtastriola + MES + LES; MS vs. juxtastriola + MES, P < 0.0001 in all cases. MS vs. LS + LES, P < 0.001. Total cells: LES vs. MS + MES; juxtastriola vs. MS + MES; MES vs. MS + LS, P < 0.0001 in all cases. LES vs. LS, P < 0.05. Synaptic endings: MS vs. MES, P < 0.0001. MES vs. juxtastriola + LS, P < 0.0005 in all cases. LES vs. MES, P < 0.005. Endings/hair cell: MS vs. MES, P < 0.001. MS vs. juxtastriola, P < 0.0005. LS vs. MES, P < 0.001. LS vs. juxtastriola, P < 0.005. MS vs. LES, P < 0.05.

four typical striolar afferents (Fig. 9a,b,e,f) is shown in Figure 10. Striolar afferents supplying the outer rows of the medial striola largely or exclusively contacted Type B and Type C hair cells. For any single afferent, the numbers of these hair cell types were inversely correlated, with some afferents innervating large numbers of Type C (Fig. 10a) and others large numbers of Type B hair cells (Fig. 10b). Afferents innervating the central or lateral striola innervated a complex mixture of all four hair cell types (Fig. 10c). Striolar afferents with thin parent axons innervated the central portion of the striolar region and contacted relatively large numbers of Type E hair cells, often of opposing morphological polarities (Fig. 10d).

The relative percentage of each hair cell type innervated by all 32 fully reconstructed striolar afferents is illustrated in Figure 11. The afferents are ordered by macular location, with afferents to the left and right of the figure supplying the medial and lateral striolar region, respectively. Several important points are evident from this figure. First, with the exception of afferents supplying the central striola, striolar afferents largely innervated Type B and Type C hair cells. This was especially true for the 16/32 afferents that supplied the outer rows of the medial and lateral striola, in which Type B and Type C hair cells made up 70 to 100% of the total innervation. Second, afferents supplying other regions of the medial and lateral striola innervated fewer Type B and larger numbers of Type E and Type F hair cells. Even in these afferents, however, Type C cells made up the majority of innervated hair cells. This was true for all but three afferents supplying the most central region of the striola. These three afferents innervated more Type E hair cells than any other hair cell type. Finally, the number of Type F hair cells contacted by a striolar afferent was small, seldom exceeding 10% of its total innervation.

DISCUSSION

Nature of labeled processes

The HRP techniques used here can potentially label sympathetic and efferent axons as well as afferent axons. We therefore sectioned the central processes of the former axons medial to their cell bodies to allow the peripheral processes of these fibers to degenerate before labeling the peripheral terminations of vestibular afferents with HRP. Two observations indicate that this procedure was successful. First, fine (< 0.5 μm) unmyelinated fibers were consistently seen in normal but not nerve-sectioned animals. These fibers, which innervate large numbers of capillaries

outside the boundaries of the sensory macula, are assumed to be sympathetic neurons (Lindeman, '69; Dunn, '76). Second, degenerated axon profiles, assumed to be the remnants of myelinated efferent neurons, were seen in nerve-sectioned but not normal animals. Somewhat surprisingly, the axon diameter of degenerated fibers was not significantly different from that of normal myelinated fibers. In previous studies, the fiber diameters of efferent neurons have been reported to be thinner than those of afferent neurons (Robbins et al., '67; Gacek, '84). The number of degenerated fibers in the anterior nerve was also somewhat higher than expected, being similar to the number of brainstem efferent neurons reported to innervate each vestibular labyrinth (Will, '82). This disparity probably reflects the collateralization of efferent neurons within the vestibular nerve.

Afferent classes

Vestibular afferents in the chinchilla and squirrel monkey have previously been classified into calyx, bouton, and dimorphic classes depending upon whether they terminate in calyx endings, bouton endings, or a mixture of both types of endings (Fernandez et al., '88, '90, '91). Vestibular afferents in lower vertebrates, unlike those of mammals, terminate only in noncalyceal endings and innervate only Type II hair cells (Honrubia et al., '81, '89; Baird and Lewis, '86; Boyle et al., '91; Myers and Lewis, '91). Like afferents in mammalian preparations, however, afferents in central and peripheral epithelial regions differ in the diameter of their parent axons, the size of their terminal fields, the number of their synaptic endings, and the number of hair cells that they innervate. In the utricle, these differences are associated with the striola, a circumscribed central region, and a broader peripheral or extrastriolar zone. Afferents in close proximity to the striola, including those in both the medial juxtastriola and the lateral extrastriola, are transitional in their properties.

The number of striolar afferents was significantly larger and the number of extrastriolar and juxtastricular afferents significantly smaller than that expected on an areal basis. Because the latter afferents are thin, they may be more difficult to label. To investigate the role of axon diameter, we sorted labeled afferents on the basis of size into 0.5 μm bins, starting at the thin end of the spectrum. For each bin, we determined the proportions of labeled afferents that were striolar (p_S), juxtastricular (p_J), medial (p_{MES}), and lateral extrastriolar (p_{LES}). The proportion of all afferents (p_T) whose size fell within the same bin was obtained from

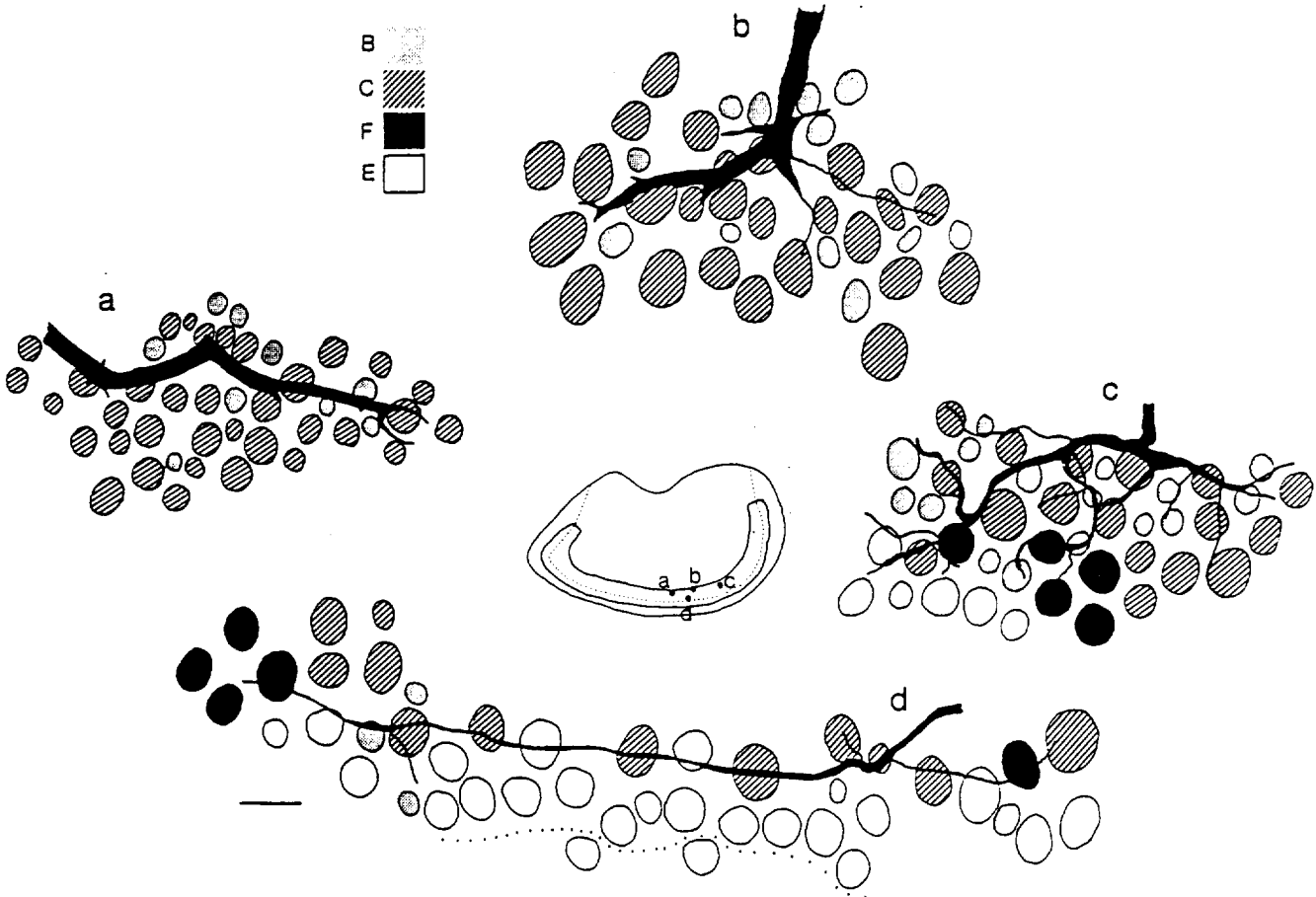


Fig. 10. a-d: Distribution of innervated hair cell types for four afferents illustrated in the previous figure, with macular locations indicated on a standard surface map of the utricular macula (inset). Dotted line in drawing d indicates the reversal of hair cell polarization. B, Type B; C, Type C; E, Type E; F, Type F. Bar = 10 μ m.

our histogram of axon diameter in normal material, correcting for the presence of efferent fibers. The individual proportions (p_s , p_j , p_{MES} , and p_{LES}) were then multiplied by the overall proportion p_T . By summing each of the three products over all bins, we obtained estimates of the proportions of the three afferent classes corrected for differences in their axon diameters. The corrected proportions were striolar units, 12.5%; juxtastriolar units, 8.6%; medial extrastriola, 72.8%; and lateral extrastriolar units, 5.8%. As expected, the correction results in an increase in the relative proportion of thin afferents. The result is a large increase in the percentage of medial extrastriolar and smaller decreases in the percentage of striolar, juxtastriolar, and lateral extrastriolar afferents (see Table 3).

Regional organization of the utricular macula

As in the chinchilla (Fernandez et al., '90), the utricular macula of the bullfrog can be divided into three zones: the striola, the juxtastriola, and extrastriola. In both species, the striola is characterized by the presence of widely spaced hair cells. In addition, hair cells in the amphibian striola possess distinctive hair bundle morphology (Lewis and Li, '75) and have unique macular distributions (Baird, '92, '93a). There is an abrupt transition in morphology between the striola and juxtastriola, and few afferents innervate

both zones. In contrast, no morphological boundary exists between the juxtastriola and the extrastriola. Rather, the distinction between the latter two zones is based solely on differences in their afferent innervation patterns. It is probably for this reason that a separate juxtastriolar zone in the utricle has only recently been recognized (Fernandez et al., '90).

The three macular zones in the utricle differ in the kinds of afferents they receive. When striolar and medial extrastriolar afferents are compared, the former have thicker axons, larger terminal fields, more synaptic endings, and innervate larger numbers of hair cells. Afferent morphology in the juxtastriola is transitional between that of the other two zones and strongly resembles that seen in the lateral extrastriola, suggesting that the morphological characteristics of afferents is correlated with their relative proximity to the striolar region. Juxtastriolar afferents are similar to striolar afferents in having few subepithelial bifurcations, large terminal fields oriented parallel to the striola, and contacting many hair cells. Unlike striolar afferents, they have thin parent axons, lack specialized synaptic endings, and possess fewer synaptic endings per hair cell. In the latter respects, juxtastriolar afferents resemble afferents in the medial extrastriola. Juxtastriolar afferents are also unique in that they enter the sensory epithelium and travel

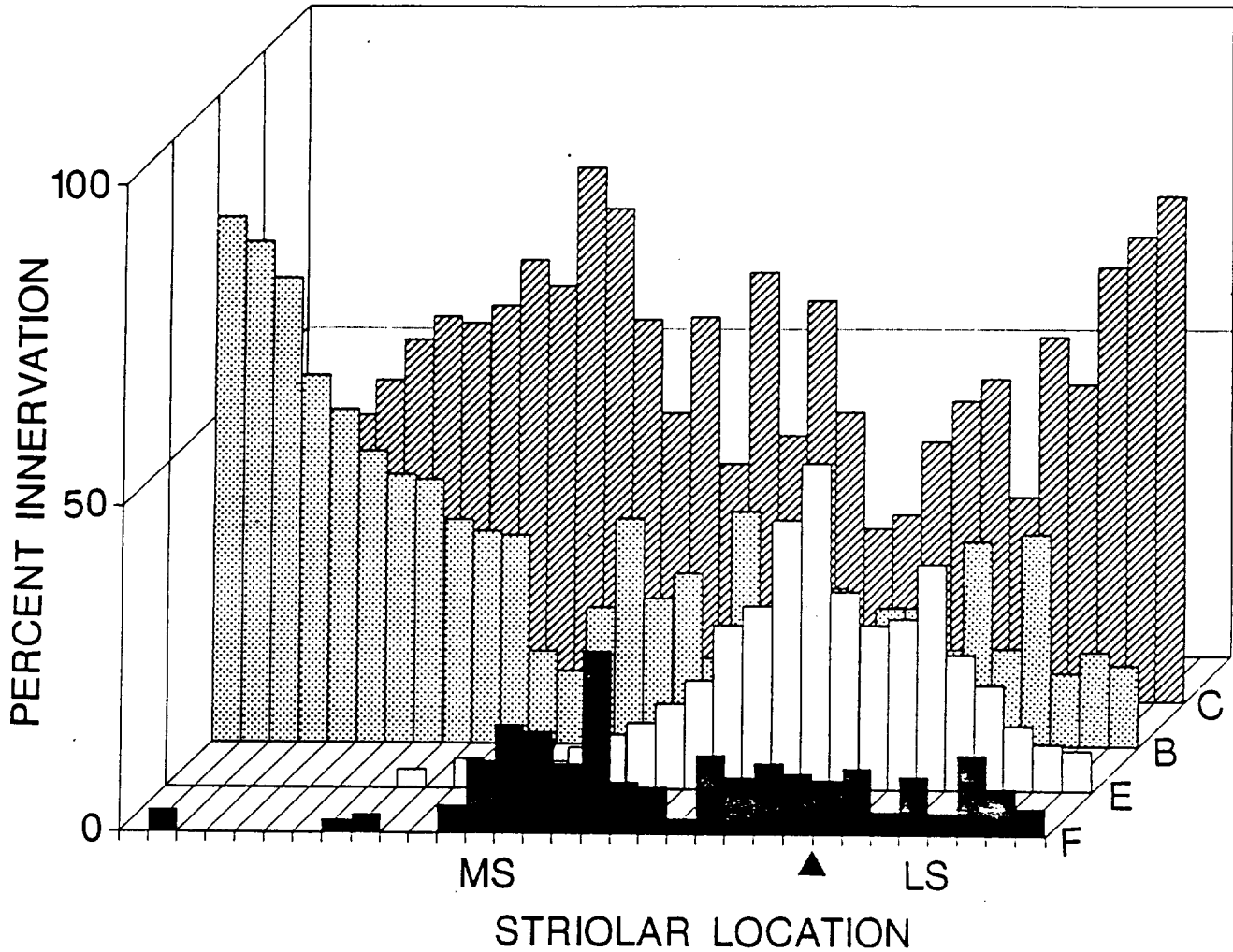


Fig. 11. Bar graph of relative percentage of each hair cell type innervated by 32 fully reconstructed striolar afferents. Afferents are ordered by macular location, with afferents to the left and right of the pointer supplying the medial and lateral striola, respectively. MS, medial striola; LS, lateral striola. B, Type B; C, Type C; E, Type E; F, Type F.

for relatively long distances without making synaptic contact with hair cells.

The striola and extrastriola can be divided into four topographic areas whose hair cells differ in the morphological polarization of their hair bundles (Lindeman, '67; Wersall and Bagger-Sjoberg, '74). By and large, regional differences among striolar afferents in the four quadrants of the macula are small. In particular, afferents in anteromedial and anterolateral regions did not differ in axon size and terminal morphology from afferents in other macular regions. This finding is in contrast to the results of Fernandez et al. ('90) in the chinchilla. The significance of this difference is unclear. As Goldberg et al. ('90b) point out, the discharge properties of afferents destined for the anterior curvature are not significantly different from afferents destined for more posterior locations.

While there are obvious parallels in the organization of the utricular macula in amphibians and mammals, there are also some significant differences. The most obvious of these is the fact that the striolar region in the bullfrog, unlike that of mammals (Lindeman, '69; Wersall and

Bagger-Sjoberg, '74; Fernandez et al., '90), is located asymmetrically. This region also occupies a significantly larger fraction of the sensory epithelium, both by area and percentage of innervation, than in the mammal (20% and 8%, respectively). As afferents excited by ipsilateral head tilts innervate the medial portions of the utricular macula whereas those excited by contralateral head tilts supply more lateral regions, this would suggest that most afferents in the bullfrog utricle should be excited by ipsilateral, as compared with contralateral, head tilts. A similar predominance is seen in the cat (Loe et al., '73) and monkey (Fernandez et al., '72; Fernandez and Goldberg, '76a). In the chinchilla, however, afferents excited by ipsilateral and contralateral head tilts are observed with approximately equal frequency (Goldberg et al., '90b).

Several other differences between amphibians and mammals are also evident. Subepithelial bifurcations of utricular afferents are more common in the chinchilla, while regional differences in the innervation patterns of utricular afferents are more striking in the bullfrog, particularly in the juxta-striolar zone. In addition, there is more cross-

over between macular zones in the bullfrog than in the chinchilla. This is particularly true for juxtastricular and lateral striolar afferents. Hair cell density, while similar in the amphibian and mammalian striola, is significantly higher in the lateral extrastricular region of the bullfrog utriculus. This may partially compensate for the relatively small area of this region relative to the medial extrastricular.

Afferent branching patterns

The terminal fields of afferents in the utricular macula are extremely compact. Afferents destined for the medial extrastricular seldom bifurcate below the sensory epithelium and, if so, contact contiguous or closely adjacent groups of hair cells. Moreover, the terminal field areas of these afferents show little regional variation, and their most distal synaptic endings are seldom $>25 \mu\text{m}$ from their parent axons. Terminal fields in the juxtastricular and striolar regions are significantly larger than those in medial extrastricular regions. The terminal fields of these afferents, however, are still relatively compact, never extending $>75 \mu\text{m}$ from their parent axons. These circumscribed terminal fields suggest that utricular afferents have a single site of spike initiation (Goldberg et al., '84).

The size and orientation of terminal fields help to ensure that most utricular afferents contact hair cells with similar morphological polarization vectors. In the medial extrastricular and juxtastricular, for example, the long axes of the terminal fields of most utricular afferents are oriented toward the striola, ensuring that they contact hair cells with nearly identical morphological polarization vectors. Afferents destined for the striolar region have terminal fields oriented parallel with the striola. The relatively large size of these fields makes it likely that individual striolar afferents supply hair cells with slightly different hair bundle orientations. As has been shown previously (Fernandez et al., '72), however, such an arrangement should have only a small influence on an afferent's sensitivity or directional properties. Obviously, an afferent's sensitivity would be reduced if it were to innervate oppositely polarized hair cells. This can only occur within the striola, which contains the boundary separating hair cells of opposing polarities (Lindeman, '67; Wersall and Bagger-Sjoberg, '74). Because extrastricular and juxtastricular afferents do not cross the striola, there is no possibility that they can contact functionally opposed hair cells. Within the striola, the terminal fields of afferents are largely restricted in their innervation to the medial or the lateral side of the striolar zone, preventing this from occurring for these afferents as well.

The degree of complexity of striolar and extrastricular afferents in the bullfrog is exactly opposite to that observed in mammals, in which central fields are simple and peripheral fields are complex (Fernandez et al., '90). Our results are, however, in good agreement with the results of morphophysiological studies in the bullfrog (Myers and Lewis, '91) and toadfish (Boyle et al., '91) semicircular canals. The reason for this discrepancy is obscure. Interestingly, the regional organization of the vestibular endorgans in lower and higher vertebrates is similar, with afferents innervating the central zone having higher gains and more phasic response dynamics than those supplying more peripheral regions. This suggests that sensitivity and response dynamics of vestibular afferents are determined not by differences in terminal morphology but rather are determined by other presynaptic (Goldberg et al., '85, '90b; Baird et al., '88) and postsynaptic (Goldberg et al., '84) transduction mecha-

nisms that vary as one proceeds from central to peripheral zones. These properties may be determined, at least in the otolith organs, by differences in the comparative transduction mechanisms of hair cell types with unique macular distributions (see below).

Synaptic morphology

The great majority ($>98\%$) of afferents in the mammalian utriculus possess calyceal endings (Goldberg et al., '90b). By contrast, afferents in the bullfrog utriculus uniformly possess noncalyceal endings. The great majority of these endings are en passant or terminal bouton-like endings. However, many afferents, especially in the striolar region, had club-like or claw-like synaptic endings. These endings are similar in morphology to those reported by Honrubia et al. ('89) and Boyle et al. ('91) in the bullfrog and toadfish semicircular canals. These endings, unlike calyceal endings, did not completely surround the basolateral surface of hair cells. Moreover, they were always associated with bouton-like endings and were largely restricted to the central, or striolar, region. They are, however, reminiscent of the calyceal endings seen in higher vertebrates in one major respect. Like calyceal endings, they were always found at the end of relatively thick branches, whereas bouton-like endings were located on thinner collaterals. The precise significance of this arrangement is unclear.

Relationship of afferent innervation patterns to hair cell types

The bullfrog, unlike the mammal, possesses only Type II hair cells. These hair cells have, however, a number of distinctive hair bundle morphologies (Lewis and Li, '75). Moreover, they have recently been shown to differ markedly in their responses to intracellular current and hair bundle displacement (Baird, '92, '93a,b). Recent studies have shown that the tallest stereocilia of Type I and Type II hair cells in mammals also display regional variations in morphology (Lapeyre et al., '92). It is not yet known whether these regional variations are associated with differences in hair bundle physiology. Studies have shown, however, that Type II hair cells in different regions of the guinea pig utriculus and semicircular canals also differ in their lectin binding properties (Baird et al., '93).

The terminal fields of afferents are largely restricted to distinct macular zones. One consequence of this is that extrastricular and juxtastricular afferents largely or exclusively innervate Type B hair cells. These are the only afferents to innervate a single hair cell type. By contrast, striolar afferents innervate a complex mixture of four hair cell types. The type of hair cells innervated by striolar afferents is correlated with the macular entrance of their parent axons. This is a consequence of the restricted terminal fields of these afferents and the restricted macular distributions of hair cell types (Baird, '92, '93a). Afferents supplying the outer rows of the striola innervate large numbers of Type B and Type C hair cells. Afferents innervating more central striolar rows, on the other hand, contact a complex mixture of four hair cell types. A small number of striolar afferents, with thin parent axons, supplies only the innermost rows of the striola, contacting relatively large numbers of Type E and Type F hair cells. This segregation of input to different afferent classes lends support to the idea that differences in afferent sensitivities and response dynamics may largely be determined by

differences in the transduction mechanisms of their innervated hair cells (Baird, '92, '93a,b).

Relation to morphophysiological studies of otolith afferents

An attempt was made to correlate the results of this study with the results of previous physiological (Loe et al., '73; Macadar et al., '75; Blanks and Precht, '76; Fernandez and Goldberg, '76a,b; Caston et al., '77; Goldberg et al., '90a) and morphophysiological (Goldberg et al., '85; Baird and Lewis, '86; Goldberg et al., '90b; Myers and Lewis, '91) studies of otolith afferents. In lower vertebrates, afferents supplying the vestibular otolith organs have been shown to possess either gravitational or vibration sensitivity (Macadar et al., '75; Blanks and Precht, '76; Caston et al., '77; Baird and Lewis, '86). Afferents with gravitational sensitivity have been further classified into three classes according to their responses to head tilt. Tonic gravity afferents respond to head position, *phasic gravity* afferents respond to head velocity, and phasic-tonic afferents respond to both head position and velocity. In mammals, otolith afferents do not exhibit purely phasic behavior and do not possess sensitivity to substrate-borne vibration (Loe et al., '73; Fernandez and Goldberg, '76a; Anderson et al., '78).

Morphophysiological studies in the bullfrog have shown that the response dynamics of utricular afferents are correlated with the macular location and hair bundle morphology of their innervated hair cells (Baird and Lewis, '86; Myers and Lewis, '91). Tonic gravity afferents, for example, contact hair cells in the extrastriolar and juxtastriolar regions. These hair cells are known from previous studies to be Type B (Lewis and Li, '75). The remaining afferents contact hair cells in the striolar region. Afferents with phasic and phasic-tonic gravity sensitivity have thick parent axons. They also tend to innervate more hair cells in the inner striolar rows than afferents with phasic-tonic sensitivity, suggesting that phasic-tonic afferents owned their head position sensitivity to Type C hair cells and their head velocity sensitivity to Type F hair cells (Baird and Lewis, '86). Our present results suggest that this is unlikely. Type F hair cells, for example, represent only a small percentage of the total innervation of striolar afferents. Striolar afferents largely innervate Type B and Type C hair cells, particularly on the outer striolar rows. Moreover, the number of Type B and Type C hair cells innervated by striolar afferents is inversely correlated. This finding suggests that striolar afferents with varying degrees of tonic and phasic gravity sensitivity differ in the number of Type B and Type C hair cells they contact. This hypothesis is supported by the results of our recent hair cell studies, which indicate that Type B cells, whether located in the striolar or extrastriolar region, are sensitive only to low frequencies and exhibit tonic response dynamics to hair bundle displacement (Baird, '92, '93a,b). Type C hair cells, on the other hand, adapt rapidly to hair bundle displacement, suggesting that they encode head velocity rather than head position. Under this hypothesis, tonic and phasic gravity sensitivity would be conferred by nonadapting Type B and adapting Type C hair cells, respectively.

Striolar afferents with vibratory sensitivity have thin parent axons and innervate large numbers of hair cells in the innermost striolar rows (Baird and Lewis, '86). Hair cells in these rows are known from previous studies to be Type E (Lewis and Li, '75). More recent studies have shown that these hair cells are the only hair cell type in the

bullfrog utricle to exhibit electrical resonance (Baird et al., '92, '93a). We therefore hypothesize that vibratory afferents owe their response properties to the electrical response properties of Type E hair cells. These afferents, unlike other striolar afferents, often innervate hair cells of opposing polarities and are presumably more interested in encoding stimulus frequency than in encoding stimulus amplitude and direction.

Our results do not indicate a clear physiological role for Type F hair cells. One possibility is indicated by physiological (Macadar et al., '75) and morphophysiological (Baird and Lewis, '86) studies indicating that phasic gravity afferents in the utricle can be further divided into slow and fast varieties. The responses of slow phasic afferents initially resemble phasic-tonic afferents, exhibiting tonic responses to head position that eventually revert to prestimulus levels. It is possible that input from Type F hair cells may subtly modify the response dynamics of phasic gravity afferents. This is supported by our recent hair cell studies, which indicate that Type F hair cells possess high frequency sensitivity but, like Type B hair cells, are slowly adapting. The ratio of Type C and Type F cells may therefore be important for determining the response dynamics of phasic gravity afferents, i.e., the response dynamics of phasic gravity afferents may be determined by the adaptation kinetics of their innervated hair cells. Because Type F hair cells tend to be innervated by afferents that also innervate large numbers of Type E hair cells, they may also confer gravitational sensitivity upon vibratory afferents. Afferents with both gravitational and vibrational sensitivity have been shown to exist in previous morphophysiological studies (Baird and Lewis, '86).

ACKNOWLEDGMENTS

We are indebted to Ms. Beverly Smith for manuscript preparation. Funding for this work was provided by National Institute of Deafness and Communicative Disorders grant DC-00355, by National Aeronautics and Space Administration grant NCC 2-651, and by grants from the Oregon Lions Sight and Hearing Foundation.

LITERATURE CITED

- Adams, J.C. (1977) Technical considerations on the use of horseradish peroxidase as a neuronal marker. *J. Neurosci.* 2:141-145.
- Anderson, J.H., R.H.I. Blanks, and W. Precht (1978) Response characteristics of semicircular canal and otolith systems in cat. I. Dynamic responses of primary vestibular fibers. *Exp. Brain Res.* 32:491-507.
- Baird, R.A. (1992) Morphological and electrophysiological properties of hair cells in the bullfrog utricle. *Ann. NY Acad. Sci.* 656:12-26.
- Baird, R.A. (1993a) Comparative transduction and tuning mechanisms of hair cells in the bullfrog utricle. I. Responses to intracellular current. *J. Neurophysiol.* (*in press*).
- Baird, R.A. (1993b) Comparative transduction and tuning mechanisms of hair cells in the bullfrog utricle. II. Sensitivity and response dynamics to mechanical displacement. *J. Neurophysiol.* (*in press*).
- Baird, R.A., and E.R. Lewis (1986) Correspondences between afferent innervation patterns and response dynamics in the bullfrog utricle and lagena. *Brain Res.* 369:48-64.
- Baird, R.A., and N.R. Schuff (1991) Transduction mechanisms of hair cells in the bullfrog utricle. *Assoc. Res. Otolaryngol. Abstr.* 14:38.
- Baird, R.A., G. Desmadryl, C. Fernandez, and J.M. Goldberg (1988) The vestibular nerve of the chinchilla. II. Relation between afferent response properties and peripheral innervation patterns in the semicircular canals. *J. Neurophysiol.* 60:182-203.
- Baird, R.A., N.A. Schuff, and J. Bancroft (1993) Lectin binding patterns of vestibular hair cells. *Hear. Res.* 65:151-153.

- Blanks, R.H.I., and W. Precht (1976) Functional characterization of primary vestibular afferents in the frog. *Exp. Brain Res.* 25:369-390.
- Boyle, R., J.P. Carey, and S.M. Highstein (1991) Morphological correlates of response dynamics and efferent stimulation in horizontal semicircular canal afferents of the toadfish, *Opsanus tau*. *J. Neurophysiol.* 66:1504-1521.
- Caston, J., W. Precht, and R.H.I. Blanks (1977) Response characteristics of frog's lagenar afferents to natural stimulation. *J. Comp. Physiol.* 118:273-289.
- Dunn, R.F. (1978) Nerve fibers of the eighth nerve and their distribution to the sensory nerves of the inner ear in the bullfrog. *J. Comp. Neurol.* 182:621-636.
- Fernandez, C., and J.M. Goldberg (1976a) Physiology of peripheral neurons innervating otolith organs of the squirrel monkey. I. Response to static tilts and to long-duration centrifugal force. *J. Neurophysiol.* 39:970-984.
- Fernandez, C., and J.M. Goldberg (1976b) Physiology of peripheral neurons innervating otolith organs of the squirrel monkey. III. Response dynamics. *J. Neurophysiol.* 39:995-1008.
- Fernandez, C., J.M. Goldberg, and W.K. Abend (1972) Response to static tilts of peripheral neurons innervating otolith organs of the squirrel monkey. *J. Neurophysiol.* 35:978-997.
- Fernandez, C., R.A. Baird, and J.M. Goldberg (1988) The vestibular nerve of the chinchilla. I. Peripheral innervation patterns in the horizontal and superior semicircular canals. *J. Neurophysiol.* 60:167-181.
- Fernandez, C., J.M. Goldberg, and R.A. Baird (1990) The vestibular nerve of the chinchilla. III. Peripheral innervation patterns in the utricular macula. *J. Neurophysiol.* 63:767-780.
- Gacek, R.R. (1984) Efferent innervation of the labyrinth. *Am. J. Otolaryngol.* 5:206-224.
- Goldberg, J.M., C.E. Smith, and C. Fernandez (1984) The relation between discharge regularity and responses to externally applied galvanic currents in vestibular-nerve afferents of the squirrel monkey. *J. Neurophysiol.* 51:1236-1256.
- Goldberg, J.M., R.A. Baird, and C. Fernandez (1985) Morphophysiological studies of the mammalian vestibular labyrinth. In M.J. Correia and A.A. Perachio (eds): *Progress in Clinical and Basic Research*. Vol. 176: Contemporary Sensory Neurobiology. New York: Alan R. Liss, pp. 231-245.
- Goldberg, J.M., G. Desmadryl, R.A. Baird, and C. Fernandez (1990a) The vestibular nerve in the chinchilla. IV. Discharge properties of utricular afferents. *J. Neurophysiol.* 63:781-790.
- Goldberg, J.M., G. Desmadryl, R.A. Baird, and C. Fernandez (1990b) The vestibular nerve in the chinchilla. V. Relation between afferent response properties and peripheral innervation patterns in the utricular macula. *J. Neurophysiol.* 63:791-804.
- Hillman, D.E., and J.W. McLaren (1979) Displacement configuration of semicircular canal cupulae. *Neuroscience* 4:1989-2000.
- Honrubia, V., S.T. Sitko, J. Kimm, W. Betts, and I.R. Schwartz (1981) Physiological and anatomical characteristics of primary vestibular afferent neurons in the bullfrog. *Int. J. Neurosci.* 15:197-206.
- Honrubia, V., L.F. Hoffman, S.T. Sitko, and I.R. Schwartz (1989) Anatomic and physiological correlates in bullfrog vestibular nerve. *J. Neurophysiol.* 61:688-701.
- Keefer, D.A., W.B. Spatz, and U. Misgeld (1976) Golgi-like staining of neocortical neurons using retrogradely transported horseradish peroxidase. *Neurosci. Lett.* 3:233-237.
- Lapeyre, P., A. Guilhaume, and Y. Cazals (1992) Differences in hair bundles associated with type I and type II vestibular hair cells of the guinea pig sacculle. *Acta Otolaryngol. (Stockh.)* 112:635-642.
- Lewis, E.R., and C.W. Li (1975) Hair cell types and distributions in the otolithic and auditory organs of the bullfrog. *Brain Res.* 83:35-50.
- Lewis, E.R., R.A. Baird, E.L. Leverenz, and H. Koyama (1982) Inner ear: Dye injection reveals peripheral origins of specific sensitivities. *Science* 215:1641-1643.
- Lim, D.J. (1976) Morphological and physiological correlates in cochlear and vestibular sensory epithelia. In O. Jahari and R.P. Becker (eds): *Scanning Electron Microscopy/1976/V*. Chicago: IIT Research Institute, pp. 269-276.
- Lindeman, H.H. (1969) Studies on the morphology of the sensory regions of the vestibular apparatus. *Ergeb. Anat. Entwicklungsgesch.* 42:1-113.
- Loe, P.R., D.L. Tomko, and G. Werner (1973) The neural signal of angular head position in primary afferent vestibular nerve axons. *J. Physiol. (Lond.)* 230:29-50.
- Lorente de N6, R. (1926) Études sur l'anatomie et la physiologie du labyrinthe de l'oreille et du VIII^e nerf. Deuxieme partie. Quelques données au sujet de l'anatomie des organes sensoriels du labyrinthe. *Trab. Lab. Invest. Biol. Univ. Madrid.* 24:53-153.
- Macadar, O., G.E. Wolfe, D.P. O'Leary, and J.P. Segundo (1975) Response of the elasmobranch utricle to maintained spatial orientation, transitions, and jitter. *Exp. Brain Res.* 22:1-22.
- McLaren, J.W., and D.E. Hillman (1979) Displacement of the semicircular canal cupula during sinusoidal rotation. *Neuroscience* 4:2001-200.
- Miller, R.G. Jr. (1977) Developments in multiple comparisons, 1966-1977. *J. Am. Stat. Assoc.* 72:779-788.
- Myers, S.F., and E.R. Lewis (1991) Vestibular afferent responses to micro-rotational stimuli. *Brain Res.* 543:36-44.
- O'Leary, D.P., R.F. Dunn, and V. Honrubia (1976) Analysis of afferent responses from isolated semicircular canal of the guitarfish using rotational acceleration white-noise inputs. I. Correlation of response dynamics with receptor innervation. *J. Neurophysiol.* 39:631-644.
- Poljak, S. (1927) Über die Nervenendigungen in den vestibulären Sinnesendstellen bei den Säugetieren. *Z. Anat. Entwicklungsgesch.* 84:131-144.
- Ramón y Cajal, S. (1908) Terminacion periferica del nervio acustico del las aves. *Trab. Lab. Invest. Biol. Univ. Madrid* 6:161-176.
- Ramón y Cajal, S. (1909) Histologie du Système Nerveux de l'Homme et des Vertebres, Vol. I. Paris: Maloine.
- Robbins, R.G., R.S. Bauknight, and V. Honrubia (1967) Anatomical distribution of efferent fibers in the VIIIth cranial nerve of the bullfrog (*Rana catesbeiana*). *Acta Otolaryngol. (Stockh.)* 64:436-448.
- Schessel, D.A., and S.M. Highstein (1981) Is transmission between the vestibular type I hair cell and its primary afferent chemical? *Ann. NY Acad. Sci.* 374:210-214.
- Schessel, D.A., R. Ginsberg, and S.M. Highstein (1991) Morphophysiology of synaptic transmission between type I hair cells and vestibular primary afferents. An intracellular study employing horseradish peroxidase in the lizard, *Calotes versicolor*. *Brain Res.* 544:1-16.
- Werner, C.F. (1933) Die Differenzierung der Maculae in Labyrinth, insbesondere bei Säugetieren. *Z. Anat. Entwicklungsgesch.* 99:696-709.
- Wersall, J., and D. Bagger-Sjoberg (1974) Morphology of the vestibular sense organs. In H.H. Kornhuber (ed): *Handbook of Sensory Physiology. Vestibular System: Basic Mechanisms*. New York: Springer-Verlag, pp. 124-170.
- West, J.R., and A.C. Black, Jr. (1979) Enhancing the anterograde movement of HRP to label sparse neuronal projections. *Neurosci. Lett.* 12:159-182.
- Will, U. (1982) Efferent neurons of the lateral-line system and the VIIIth cranial nerve in the brainstem of anurans. A comparative study using retrograde tracer methods. *Cell Tissue Res.* 225:673-685.